

Pultruded Textile Reinforced Concrete Structural Sections

by

Jacob Bauchmoyer

A Thesis Presented in Partial Fulfillment
of the Requirements for the Degree
Master of Science

Approved April 2017 by the
Graduate Supervisory Committee

Barzin Mobasher, Chair
Narayanan Neithalath
Subramaniam Rajan

ARIZONA STATE UNIVERSITY

May 2017

ABSTRACT

Pultrusion manufacturing technique stands at the forefront for efficient production of continuous, uniform concrete composites for use in large scale structural applications. High volume and low labor, among other benefits such as improved impregnation and better sample consistency, stand as some of the crucial advances found in automated pultrusion. These advantages introduce textile reinforced concrete (TRC) composites as a potential surrogate for wood, light gauge steel, and other common structural materials into an ever changing and broadening market of industrial grade structural sections. With the potential modifications of textile geometry, textile type, section geometry, and connection type, the options presented by TRC sections seem nearly boundless. Automated pultrusion presents the ability to manufacture many different TRC composite types in at a quickened rate opening up a new field of study of structural materials.

The objective of this study centered on two studies including the development of an automated pultrusion system for the manufacturing of TRC composites and ultimately the assessment of composites created with the pultrusion technique and their viability as a relevant structural construction material. Upon planning, fabrication, and continued use of an automated pultrusion system in Arizona State University's Structures Lab, an initial, comparative study of polypropylene microfiber composites was conducted to assess fiber reinforced concrete composites, manufactured with Filament Winding Technique, and textile reinforced concrete composites, manufactured with Automated Pultrusion Technique, in tensile and flexural mechanical response at similar reinforcement dosages.

A secondary study was then conducted to measure the mechanical behavior of carbon, polypropylene, and alkali-resistant glass TRC composites and explore the response of full scale TRC structural shapes, including angle and channel sections. Finally, a study was conducted on the connection type for large scale TRC composite structural sections in tension and compression testing.

TABLE OF CONTENTS

	Page
LIST OF TABLES	vii
LIST OF FIGURES	viii
CHAPTER	
1. INTRODUCTION	1
1.1 Overview.....	1
1.2 Material Market	3
1.3 Concrete Mechanics.....	7
1.4 Fiber Reinforced Composites	8
1.5 Textile Reinforced Composites.....	9
1.6 Objective.....	10
2. DEVELOPMENT OF AN AUTOMATED PULTRUSION SYSTEM FOR THE MANUFACTURING OF CONTINUOUS TEXTILE REINFORCED CONCRETE COMPOSITES.....	11
2.1 Overview.....	11
2.2 Impregnation - Spool, Water & Paste Bath, and DC Rollers.....	12
2.3 Pulling Mechanism	16
2.3.1 Overview	16
2.3.2 Setup	16

CHAPTER	Page
2.3.3 Pneumatic System	18
2.3.4 Air Solenoids & LabView VI	19
2.4 Press	21
2.5 Sample Production	22
2.5.1 Mix Design.....	22
2.5.2 Textile Volume Fraction	23
2.5.3 Plate Production	24
2.5.4 Structural Shapes	25
2.6 Testing Methods.....	27
2.6.1 Tension.....	27
2.6.2 Tension in Plates	27
2.6.3 Tension in Angle Sections	28
 3. COMPARATIVE ASSESSMENT OF UNIDIRECTIONAL FILAMENT WOUND FIBER REINFORCED CONCRETE VERSUS PULTRUDED TEXTILE REINFORCED CONCRETE	30
3.1 Overview.....	30
3.2 Experimental Program	30
 4. MECHANICAL PROPERTIES AND BEHAVIORS OF TEXTILE REINFORCED CONCRETE STRUCTURAL SHAPES	38

CHAPTER	Page
4.1 Overview	38
4.2 Sample Preparation	38
4.2.1 Matrix Phase	38
4.2.2 Textile Components	39
4.3 Experimental Results	42
4.3.1 Mechanical Testing	42
4.3.2 Carbon Composites	43
4.3.3 Polypropylene Composites	45
4.3.4 ARG Composites	46
4.3.5 Structural Shapes	48
5. EFFECTIVE OF CONNECTION TYPE FOR LARGE SCALE ARG TEXTILE REINFORCED CONCRETE STRUCTURAL SHAPES	55
5.1 ARG Coupon Testing	55
5.2 Type I Gripping System – One bolt/vertical bolts	56
5.3 Type II Gripping System – Two bolts per leg	57
5.4 Type III Gripping System – Six bolts per leg	59
5.5 Digital Image Correlation Analysis	61
6. CONCLUSION.....	64

CHAPTER	Page
6.1 Relevance	64
6.2 Applications	64
6.3 Future of study	65
7. REFERENCES	66
APPENDIX	Page
A POLYPROPYLENE TRC TENSION DATA	70
B TRC STRUCTURAL SHAPE GRIPPING FIXTURES.....	73
C TRC STRUCTURAL SHAPES FAILURE MODES	77

LIST OF TABLES

Table	Page
1: Mix Design of TRC Samples	23
2: Mix design for polypropylene TRC study.....	31
3: Groups of specimens of TRC developed in the study	33
4: Tension results from open weave 4% polypropylene study.....	35
5: Weight fractions per 1 kg of matrix mixture.....	39
6: Textile volume fraction for a typical TRC Plate sample (13x279x1524mm)	41
7: Mechanical response properties of pultruded TRC coupons at 1% textile reinforcement.....	47
8: Mechanical properties of TRC composites containing 1% ARG textile by volume.....	55
9: Tension Test: 1.22m Test Type III Grips	62
10: Compression Test: Type II Grip.....	63
11: Analyzed tension test results from TRC specimens.....	71
12: Analyzed flexural test results from TRC specimens	72
13: Type I Grip Diagrams.....	74
14: Type II Grip Diagrams.....	75
15: Type III Grip Diagrams.....	76
16: Failure modes of TRC angles	78
17: Failure modes of TRC channels.....	79

LIST OF FIGURES

Figure	Page
1: Typical stress strain response of unidirectional composites	9
2: Automated pultrusion system for manufacturing TRC	12
3: Textile passing through paste bath.....	14
4: Coated textile leaving the paste bath and entering the DC powered rollers.....	15
5: Schematic of pulling mechanism	16
6: Pulling mechanism used in automated pultrusion system.....	18
7: Air flow diagram of pulling mechanism	19
8: Front panel of LabView VI	19
9: Wiring diagram of air solenoid connection to NI module	20
10: Block diagram of pultrusion VI.....	21
11: Pneumatic press before pressing a plate sample	21
12: (a) Multiple plate samples cast in one session; (b) Pressing of multiple plates	25
13: Cross section of pultruded TRC angle.....	25
14: (a) stack of steel and TRC angles before pressing; (b) pressing of TRC angles.....	26
15: Tensile testing setup of TRC plate section	28
16: Tension testing setup of TRC angle on Instron load frame	29
17: (a) Open weave patterns (b) & (c) tricot weave patterns of textiles woven from MF40 microfibers.....	32
18: Comparison of LVDT and stroke response of 4.0% open weave TRC specimens.....	34
19: Comparison between 4% and 8% open weave TRC composites	35

Figure	Page
20: Stress-strain response of TRC with MF 40 textiles after 28 days of curing in tension.....	36
21: (a) Flexural response of MF40 TRC composites; (b) tensile versus flexural response	37
22: Textile volume fraction analysis.....	40
23: (a) Carbon, (b) PP, and (c) ARG textiles used to manufacture pultruded structural sections....	42
24: Direct tension and compression testing setup for pultruded TRC coupons with digital image correlation.....	43
25: (a) Tension and (b) compression stress-strain response of carbon TRC specimens	44
26: Tensile failure of carbon coupons displaying distributed cracking along length and compressive failure showing some delamination and local crushing.....	44
27: (a) Tension and (b) compression stress-strain response of PP TRC specimens	45
28: Tensile failure of PP composite showing extremely fine crack that eventually led to failure and compressive failure of PP specimen exhibiting buckling delamination	46
29: (a) Tension and (b) compression stress-strain response of ARG TRC specimens	47
30: Tensile failure of ARG coupon showing single large crack along gage length and failure in compression displaying splintering and excessive delamination between all textile layers	47
31: Comparative plot of ARG, PP, and Carbon TRC representative specimens.....	48
32: Pultruded TRC composite L and C structural sections.....	48
33: Single bolted tension test setup and (a) front facing free body diagram and (b) thickness profile free body diagram	50
34: Stress strain response and typical failure mode of single bolted tension coupons	50

Figure	Page
35: Double bolted tension test setup and (a) front facing free body diagram and (b) thickness profile free body diagram	51
36: Replicate plot of ARG specimens tested in tension with bolted end connections	52
37: Tension test of full size TRC structural L-section and C-section with bolted connections on each leg	53
38: Tensile stress-strain replicate plot of TRC angles	54
39: Comparative plot of ARG fixed and bolted coupons and structural shapes	54
40: Tensile and compressive stress strain response of ARG plate coupons	56
41: Compression specimen mounted on Instron frame with preliminary gripping system.....	57
42: (a) Tensile Stress-Strain response of channels with Type II of 3 different configurations; (b) Compressive Stress Strain response of specimens connected with Type I, Type II, and Type III ..	58
43: (a) Tensile Stress-Strain response of channels of Type II with 2 configurations and Type III gripping system (b) Tensile Stress- Strain response of angle of Type II and Type III gripping configuration.	60
44: Tensile cracking and compressive buckling of 1.22 m long TRC L sections	61
45: Pultruded TRC sandwich section	65

1. INTRODUCTION

1.1 Overview

Concrete is the most widely used construction material in the world. It is a seemingly universal building material that has extremely high compressive strength, good durability, and can easily be molded to essentially any shape. Aggregates, sand, and admixtures mixed with one of many types of cement can lead to a range of different applications within structures, from footings to structural supports and even surface texturing. The uses of concrete are virtually limitless, and with such high quantities of concrete being used in projects around the globe, improvements in any aspect of the industry are highly influential. Reinforced concrete is one such improvement that has been used for almost one hundred years. Though steel rebar is usually used in reinforced concrete, glass and polypropylene fibers are also common reinforcement in concrete and are known as fiber reinforced concrete (FRC). FRC can lead to different advantages, such as higher tensile strength and increased toughness, and some disadvantages, like difficult casting and potential variation between samples. Textile reinforced concrete (TRC) is another form of FRC that allows for support in two directions leading to more diverse applications.

The development and use of prefabricated lightweight cement panels and structural shapes is an essential component of developing sustainable construction products. Innovative reinforcement and manufacturing techniques allow for significant increase in material strain capacity, strength, ductility and thus durability. While a range of randomly distributed short fibers and continuous unidirectional fibers have been shown to be

applicable in making high performance cement composites, the use of two-dimensional reinforcing textiles have shown to be greatly effective in improving ductility, tensile and flexural strength, and toughness [1, 2, 3, 4].

The opportunity to manufacture products using an automated pultrusion system is important as various structural shapes with optimal dimensions can be produced with minimal labor and high degree of automation accuracy [5, 6]. Pultrusion therefore stands as a low-cost manufacturing technique for textile reinforced concrete (TRC) composites with improved textile-paste bond due to enhanced impregnation as compared to traditionally cast composites [7, 8, 9]. Peled and Mobasher showed pultrusion production requires less production time and sample manipulation resulting in less strength reduction from bond degradation between the fiber and matrix [10, 11]. The system presented by Peled and Mobasher showed significant potential in sample production but was limited to specific thin plate dimensions due to the winding driven nature of the process.

Industrial pultrusion systems based upon the Goldsworthy method are commonly used in thermoplastic and aluminum production today, thus it is a proven and viable method for large and complex shapes [12]. Due to its continuous operation, industrial pultrusion allows for significantly reduced manual labor when compared to traditional manufacturing techniques [13, 14]. Resin and metallic based pultruded composites are however controlled either at excessively high temperatures, or set as thermoplastics or thermosets [15, 16, 17]. Cement based composites are controlled by hydration through non-equilibrium precipitation of calcium silicate hydrates which are rheologically complex due to the multiple phases present. Excess hydrostatic pressures result in fluid and solid phase

separation. There is hence a need for alterations to the industrial production of thermosets and thermoplastic based composites to make them applicable to TRC production. Pultrusion in most industrial production lines is composed of three stations: an initial feeding section that combines matrix and reinforcement to pass through a die cast, the driving system which is typically an automated tractor or caterpillar pull, and finally a take up section in which the composite is formed into the final shape, completes curing, and is cut to size.

1.2 Material Market

The current global construction industry is heavily reliant on concrete as a core structural material throughout a widening range of project scopes. From simple floor slabs to large, pre-stressed highway girders, concrete has become the most used construction material in the world. With the efficient manufacturing industry and a high demand for concrete in structural projects, concrete is an extremely economic material as well. Its economy makes it a desirable alternative to more costly materials such as steel and timber. Equally, while concrete has a high initial carbon release during manufacturing, concrete is a significantly sustainable material based on its durability and low level of required maintenance. It is also fire and water proof and can be molded to any desired shape. It is a highly efficient material with a wide range of benefits.

Unfortunately, concrete comes with several associated costs despite its benefits. Concrete is far weaker in tension than in compression, typically by almost an entire order of magnitude. It is also a brittle material in which failure is catastrophic and sudden upon

reaching UTS. The necessity of formwork when fabricating concrete systems also adds cost to projects. The final major concern with concrete is that it can also be highly variable due to the nature of porosity and impurities. Addressing these major detriments of using concrete would open a new market to compete with the likes of other costlier and less sustainable materials like wood and light gauge (cold-formed) steel. Before delving into concrete modifications and improvements, the benefit of entering the prospective market should first be assessed by studying the competitive materials of wood and light gauge steel.

Light gauge, or cold-formed, steel is an increasingly sought structural material contributing to a growing market that is pulling from the wood industry. While design started as early as 1946 with the release of the first design specifications by the American Iron & Steel Institute (AISI), cold formed steel (CFS) came to higher prominence in 2001. More projects began turning to the previously limited use material with the NAFTA embargo clearing the way for better trade options and the AISI release of the first formal CFS design code, *North American Specification of the Design of Cold-Formed Steel Structural Members* [18]. The 2000 projections through 2004 anticipated the industry to move to a nearly \$1.2 billion market with most demand coming from commercial projects [19]. Current outlooks have shown that the now multi-billion-dollar market will likely sustain a 3.8% growth over the next five years from the commercial and residential construction industries [20]. Sheila Kovarik has illustrated that the original disconnect between the residential and commercial demand has shrunk over the last decade as residential development demand is now a \$35 billion industry with far higher interest in

CFS today than the 1990s or even the early 2000s [21]. As Kathryn Thompson presented in her 2016 CFS Economic Outlook discussion, the U.S. residential development and ownership rates are steady but ultimately lower than anticipated after the 2008 economic crisis which has led to a focus in decreasing costs of housing development [22]. This has spurred the cold formed steel industry in its bid against wood construction by reducing required material volume. This is often satisfied with CFS due to its higher structural quality and efficiency. Steel prices have also decreased recently which has further stimulated CFS demand. CFS is also versatile in a variety of structural applications, including shear walls, bearing supports, roofing, curtain walls, and many others [23, 24]. Dr. Serrette's study in 1997 gave a surge in CFS design flexibility in showing the effectiveness of CFS as the core of shear walls over plywood and traditional lumber members [25]. However, the material's driving detraction is that, even with the reduced cost of steel at the current time, it still far exceeds unit cost of concrete and wood by volume. Additionally, it is still highly vulnerable to environmental damage such as fire or flooding in which maintenance increases long term costs.

The lumber market is an extremely sturdy, albeit variable market with high prospects for the future. While the CFS market pulls from timber sales, the world import demand reached \$111 billion dollars in 2014 alone [26]. The industry also experienced an annual compound growth of 9% from 2009 through 2014. In 2014, 13.1% of China's \$22.1 billion in wood product imports were from the United States. The cost of wood fluctuates from year to year, as shown in current studies and projections, but demand typically follows a consistent growth rate that looks to continue over the next five years [27]. Prospects in

the energy industry also drive wood prices and lead to fluctuations across market quarters [28, 29]. Studies like that of Wallace, Cheung, and Williamson have shown the increased versatility of wood construction in creating multistory buildings through entirely timber construction [30]. Some wood products even offer project heights over 80 ft to allow higher flexibility in structural design [31]. However, water, fire, and environmental effects, such as termite damage, make wood structures highly vulnerable with high variation in risk throughout the United States [32]. This leads to increased risk in building wood structures that is not as present, if at all, in concrete and steel based projects.

The promise for the CFS industry is strong, but there has not been an instant switch from timber to steel as would be expected when comparing the costs and benefits of each. The cause is likely the dichotomy of structural design efficiency versus material economy. The significant increases in stiffness and strength found in CFS versus wood allows for more freedom in structural design, allowing for modifications such as larger column spacing that creates larger serviceability square footage. In commercial projects like office buildings and retail markets, this is highly desirable as revenue is generated by the serviceable area. However, in residential development the improvements are to a much smaller scale due to the reduction in site footprint. Serviceability is no longer as direct as simple square footage measurement. Many home buyers or renters' decision of purchase is more dependent on aesthetic characteristics than just available area. This neutralizes many of the benefits brought by CFS and has allowed the continuation of the timber market within the residential industry. Most residential sites remain within the design capacities of wood and retain nearly identical aesthetic characteristics as those with CFS builds. Both

materials are costly, but clearly the extra benefits brought by CFS are not as sought in residences as they are in commercial construction. Therefore, the material economy of wood makes it the more common material used in residential development, despite the design efficiency, albeit increased cost, brought by CFS.

Prospects of the concrete market moving into the commercial and residential framing industry dominated by CFS and wood are much higher than would be initially anticipated. However, this prospect is dependent upon three central necessities: comparable design benefits relative to associated costs, price differences, and feasibility of manufacturing.

1.3 Concrete Mechanics

Concrete is a combination of aggregate and cement binder. Aggregates are rock and material that have been cleared of fine and organic matter to allow for controlled characterization. The aggregates are held together through the hydration of a binder which is typically a form of Portland cement. Portland cement comes in a variety of types and each type provides different benefits such as increased durability, alkali resistance, and strength gain. Portland cement is activated by hydration and typically cures to full strength within 28 days. The proportions of aggregates and cement change the properties of the dried concrete significantly, and other additives can be combined with the mixture to further improve these characteristics. Concrete is a ceramic material that is extremely strong in compression due to the bond of the aggregates and the binder, but it is also brittle with low tensile strength and strain capacity. This weakness in tension prevents its use as

a tensile load bearing material in structures which is why it is typically used in foundations, footings, and wide base or low level structures. To improve the tensile properties of concrete, the use of reinforcement within the paste matrix has become a common practice that is constantly improving and advancing.

1.4 Fiber Reinforced Composites

Composites in a broad sense are a combination of different materials that form one new material with attributes from all of the parent materials. The most commonly used composite is concrete which is composed of a cement binder and aggregate that are combined together to create a homogenous mixture. Reinforced composites are a combination of a matrix paste and a form of reinforcement that is impregnated into the matrix paste to create a bond interface that mitigates crack propagation and increases strength [33, 34, 35]. Typical reinforcements used in cementitious composites are fibers and two dimensional textiles. Fiber reinforcement can be of short or continuous nature with random or uniform distribution. Every reinforcement orientation leads to different property effects. Plain concrete follows the tensile behavior shown in region I of the stress strain response in Figure 1.1 with a period of elastic straining followed by failure after the first crack at point B. Continuous unidirectional fiber reinforced concrete (FRC) follows the complete response shown in Figure 1. After entering the plastic state in regions II and III, the fiber reinforcement bridges cracks as they form in the composite. Multiple parallel cracks form transverse to the direction of loading before the composite

enters a period of strain hardening until failure upon reaching the ultimate tensile strength at point D.

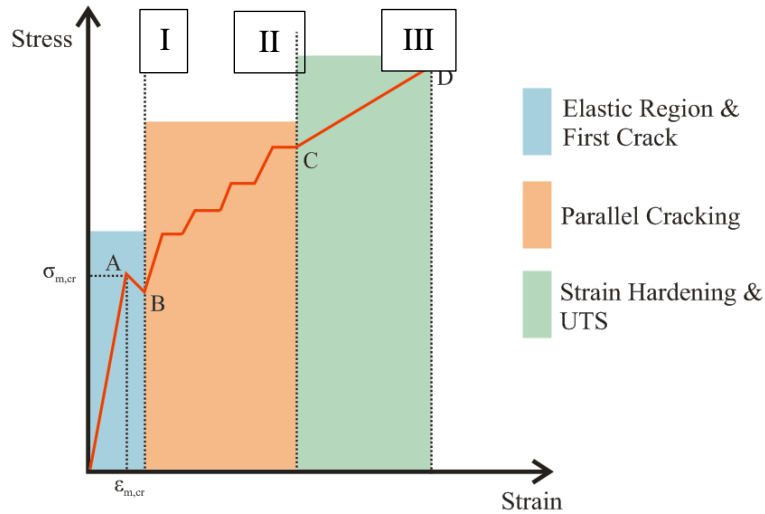


Figure 1: Typical stress strain response of unidirectional composites

1.5 Textile Reinforced Composites

While uniaxial FRC exhibits many desirable properties, one significant weakness is that strength and toughness gain are limited to the direction of the fiber reinforcement, and manufacturing of uniaxial FRC can be costly and difficult. With these limitations, the appeal for FRC as an effective design material drops. However, a significant alternative within the same mindset of FRC is textile reinforced concrete (TRC). TRC is an emerging material that exhibits many similar properties to FRC but also provides improvements in multiple aspects. While multi-axial FRC must be manufactured layer by layer, TRC makes use of two-dimensional glass or polypropylene textiles that provide support in both the loading and transverse direction upon impregnation in the cement matrix. This allows for more efficient production and consistent textile volumes within the composites. The transverse reinforcement allows for improved flexural capacity and better ductility than

FRC composites. When compared to a uniaxial FRC with the same fiber volume fraction, the limitations of TRC are a reduced percentage of fiber in the loading direction which leads to some reduction in strength despite an increase in strain capacity. Manufacturing of TRC can also be a difficult process as complete impregnation is more difficult due to the bond surface area lost by the weave of the textile.

1.6 Objective

The first objective of this thesis was to develop and construct an automated pultrusion system for the manufacturing of textile reinforced cementitious composites. A manual pultrusion system previously developed at Arizona State University and large scale industrial pultrusion techniques were used as a basis for the development of this new automated system. The system was divided into a series of stations that each serve as a component of manufacturing of textile reinforced concrete. Though commonly hydraulic, the automated system was made using pneumatic lines and automated through the use of computer-controlled air solenoids. Computer programming was required to create a virtual interface that could control the production line. The pultrusion system was constructed and preliminarily studied for fulfillment of the Barrett Honors Thesis requirement for this thesis candidate and portions of the system description in Chapter 2 are included to convey the workings of the system that lead to the phenomena seen in the second part of this thesis study [36]. The overall goal was a proof of concept that this technology can properly be fabricated and implemented to manufacture a wide range of textile reinforced cementitious composites, including plate sections and structural shapes. Manufacturing and mechanical testing of these large-scale shapes became the second part of this thesis.

2. DEVELOPMENT OF AN AUTOMATED PULTRUSION SYSTEM FOR THE MANUFACTURING OF CONTINUOUS TEXTILE REINFORCED CONCRETE COMPOSITES

2.1 Overview

Pultrusion is not a novel manufacturing technique for composite materials as aluminum extrusions and plastic pipes are produced using pultrusion techniques similar to those adopted in this project. The general production line remains generally the same from system to system [37, 38, 39]. For composites, fiber reinforcement is first pulled from a roving or spool. Different dosages of reinforcement can be used to change the composite properties such as stiffness. The reinforcement is then passed through an impregnation chamber that coats the fibers with the matrix paste of the composite. Heat is typically used to melt matrix material so that it can properly coat the reinforcement and harden as it cools. The combined composite is then passed through a dye cast that shapes the cross section while the matrix is still plastic. The composite is moved continuously through the entire system using either a tractor or caterpillar pulling mechanism near the end of the production line. The pulling mechanism grips and tows the composite as it moves through each station. At the end of the line, a saw cuts the composite to the desired length.

The automated pultrusion system consists of five central stations oriented in succession along a continuous production line. The five stations are the spool, the water and paste baths, the DC powered rollers, the pulling mechanism, and the pneumatic press. A pneumatic tractor pulling mechanism is used in this apparatus which operates through a series of air solenoids that are computer-controlled through a VI program made in

LabView. The next three sections discuss the specifications and use of each station within the pultrusion system. The system is shown below in Figure 2.

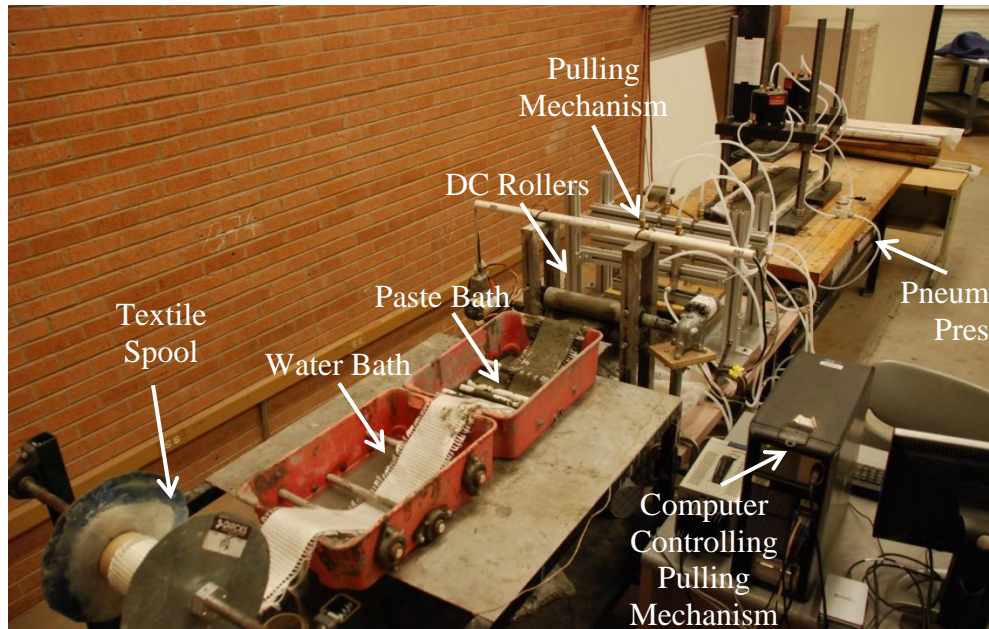


Figure 2: Automated pultrusion system for manufacturing TRC

2.2 Impregnation - Spool, Water & Paste Bath, and DC Rollers

When manufacturing TRC, textile impregnation into the matrix is a crucial concern. Without complete impregnation, the composite strength will be reduced significantly and the general material properties will be compromised due to improper stress transfer between the matrix and reinforcement. While longitudinal filaments within a textile are coated with paste similar to fiber reinforced concrete, the presence of the lateral filaments within the textile creates difficulties in effective impregnation. The two-dimensional nature of the textile requires matrix penetration into the open cells between the spaced filaments for proper impregnation.

The first station within the impregnation section of the pultrusion system is the textile spool. Winding the textile onto a spool is important as it streamlines the

manufacturing of TRC. A spool presents a clean, uniform feed of textile into the pultrusion system stations that allows for better sample production. Depending on the required sample size, the textile typically must be cut to the proper width and production length. This study included manufacturing of TRC with alkali resistant (AR) glass textile and fibrillated polypropylene (PP) textiles. When casting samples, the AR glass textile was cut to length and width from a bulk spool that was too large to mount within the system. The PP textiles were specially made to test the effect of weave pattern and were pre-cut to the proper width. They simply needed to be cut to length. When cutting textiles to length, the total length of textile to be used in all samples to be cast was left in either one or two continuous pieces to allow the pultrusion system to completely run the textile through the preparation, impregnation, towing, and laying stations until sample finishing and shaping. Extra length was left on the textile spools to provide enough length for complete sample production. The excess material can either be disposed of or salvaged and reused if it is not coated in matrix.

The second station within the impregnation line is the water and paste baths. As the textile leaves the spool it enters the water bath which is a 16"x12"x6" tub that serves to lightly wet the textile. Three 3/8" all-thread rods covered in 1/2" PVC pipe run along the 12" width of the tub and are transverse to the production line. They are oriented in a "V-shape" with the middle rod placed 2" from the bottom of the tub and the outer rods are placed 3.5" above the bottom of the tub. The textile passes over the first outer rod, under the middle rod, and over the third rod. The waterline in the bucket is even with the bottom of the middle rod casing. These rods act as contact points that skim the textile over the

water surface and maintain tension in the textile as it moves down the line. The all-thread rods are fixed to the bucket while the PVC casings are allowed to rotate freely on the rods. This lowers the friction caused by the water bath and prevents damage of the textile when passing over the rods.

Wetting of the textile is important because it prevents drying of the paste as the textile passes through the bath and allows for better matrix coating. This leads to better impregnation as the textile is able to absorb more paste. After passing through the water bath, the textile passes through the paste bath. The paste bath is designed the same as the water bath but is instead filled with matrix paste instead of water. The cement paste is the same as that of the sample casting but contains additional superplasticizer to allow for better coating of the textile. The textile passing through the paste bath is shown below in Figure 3.



Figure 3: Textile passing through paste bath

The third and final station within the impregnation line is the set of DC powered rollers. Once the textile is coated in paste, it passes through two 2" diameter 12" wide, steel rollers separated spaced 1/2" apart vertically. Figure 4 shows the coated textile entering the rollers from the paste bath. These rollers stand on two steel frames that hold them in place but allow them to rotate as the coated textile passes through them. They are each attached to a 24V DC motor that spins the roller counterclockwise. The motors are positioned opposite of each other so that the rollers spin in opposite directions. The motion and spacing of these rollers spread the paste along the textile evenly. With uniform coating, the textile will be better impregnated as all cells of the textile will be filled and the textile will remain plane within the composite.



Figure 4: Coated textile leaving the paste bath and entering the DC powered rollers

2.3 Pulling Mechanism

2.3.1 Overview

The fourth station along the pultrusion production line is the pulling mechanism. It is arguably the most important aspect to the system because the pulling mechanism is automated and drives the production forward. A tractor pull technique was used in this setup. A tractor pull is similar to a hand over hand pulling of the textile down the production line. The pulling mechanism gripped the sample and pulled it down the line before releasing it and returning to its starting position to repeat the cycle. The pulling mechanism was pneumatic and controlled by a series of air solenoids that are turned off and on with a virtual instruments (VI) program written using National Instruments LabView software.

2.3.2 Setup

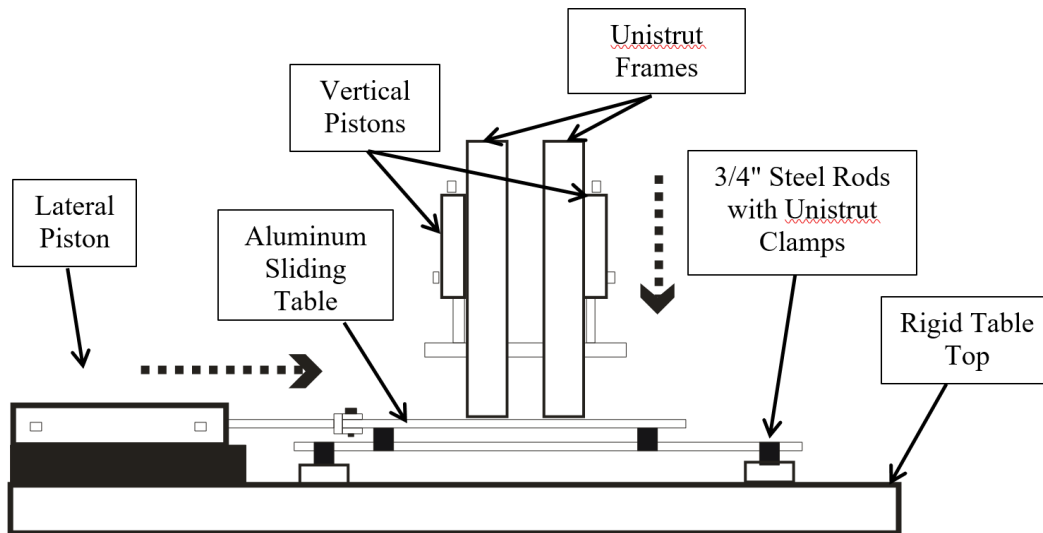


Figure 5: Schematic of pulling mechanism

As shown in Figure 5, the pulling mechanism for this system was composed of several elements that worked to create a vertical clamp that can move laterally. The base plate was an 18"x30"x0.375" aluminum sliding table rested on two 3/4" steel bars that were mounted with four steel straps connected to four 8" unistrut sections that were bolted to the production table. The steel bars were connected to the aluminum sliding table with four rollers that allowed the table to move along the bars in the direction of production with limited friction. A pneumatic piston with a 6" stroke fixed to the production table was connected to the sliding table to drive it down the production line. On the top face of the sliding table, two aluminum unistrut frames were mounted vertically. The frames consisted of four 18" T-shaped 40 mm hollow unistrut columns that were mounted along the 18" dimension of the table spaced 6" apart. They were mounted with unistrut floor angle brackets with two 26" unistrut beams connecting each pair of columns across the 30" dimension. The beams were connected to the columns with 90° angle brackets to allow for adjustment of the beams along the columns. Four pneumatic pistons with a 6" stroke were connected to each beam with steel straps and positioned to act vertically downwards. The ends of each piston were threaded to connect to a wooden board that acted as the top clamping surface for the pulling mechanism when the pistons were fully extended. The wooden board was protected with a neoprene layer to prevent water damage and increase friction. An additional neoprene-coated, wooden board was bolted to the aluminum plate to provide a high friction clamp for pulling the paste coated textiles. The pulling mechanism is shown below in Figure 6.

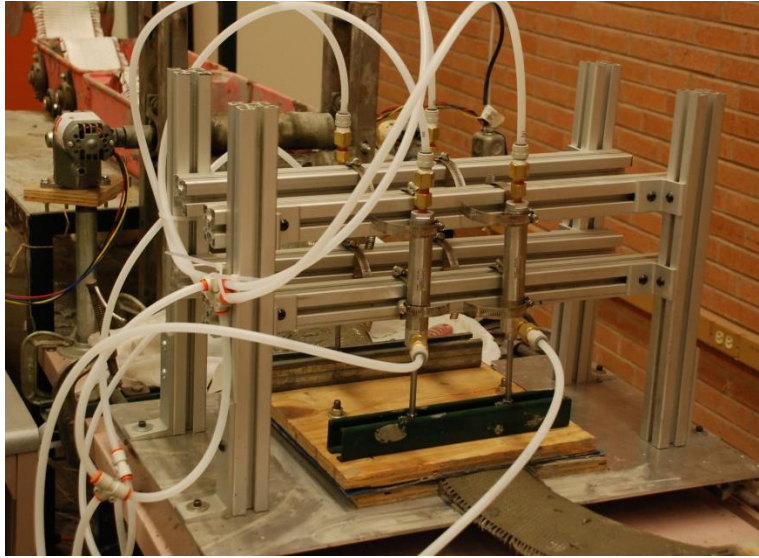


Figure 6: Pulling mechanism used in automated pultrusion system

2.3.3 Pneumatic System

The pulling mechanism used in this system is controlled through a pneumatic system that is automated through the use of computer-controlled solenoids. In the pulling mechanism's pneumatic system, the four 4" stroke pistons that move vertically to engage the clamping motion on the textile are connected to the building air pressure for inflow and vented out to allow the vertical motion. The direction of the air flow determines the motion of the pistons. Pressure is controlled through a pressure regulator that maintains a uniform pressure of about 3 psi. This allows for smooth motion and adequate gripping pressure in the clamp. The flow lines are connected between the four pistons with 3/8" plastic hosing, plastic tee connectors, and 1/4" to 3/8" NPT adapters for the pistons. The lateral piston is also connected in series with the vertical pistons to provide the horizontal movement of the pulling mechanism. The air flow diagram of the pulling mechanism is shown below in Figure 7.

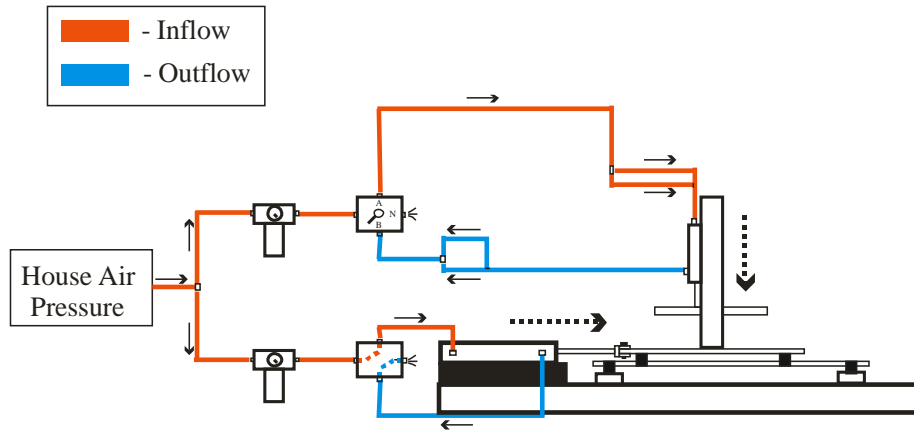


Figure 7: Air flow diagram of pulling mechanism

2.3.4 Air Solenoids & LabView VI

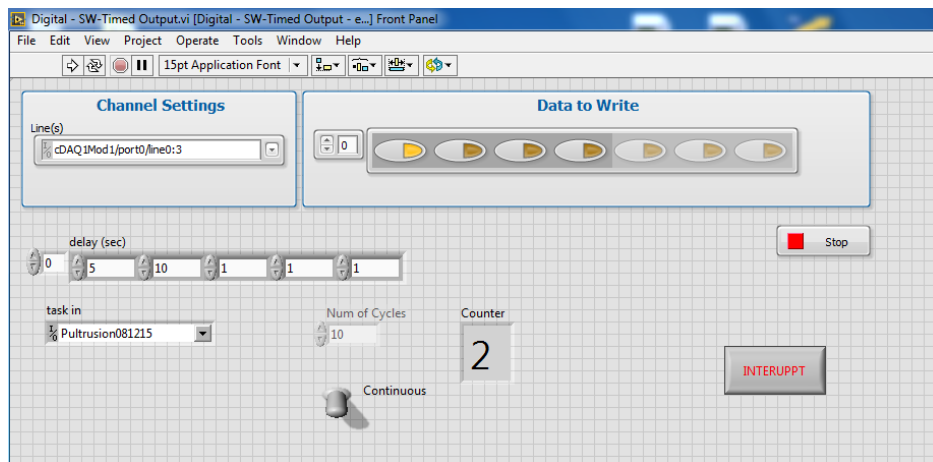


Figure 8: Front panel of LabView VI

The air solenoids act as the driving controllers for the automated pultrusion system and are turned off and on through their connection to a 24V DC power supply. A National Instruments chassis connects the 24V DC power supply and air solenoids to the computer in order to run the system. The chassis has a port connected to each solenoid that when active completes the circuit and the solenoid opens. When the port is deactivated, the solenoid closes. The wiring diagram for a single solenoid is shown in Figure 9.

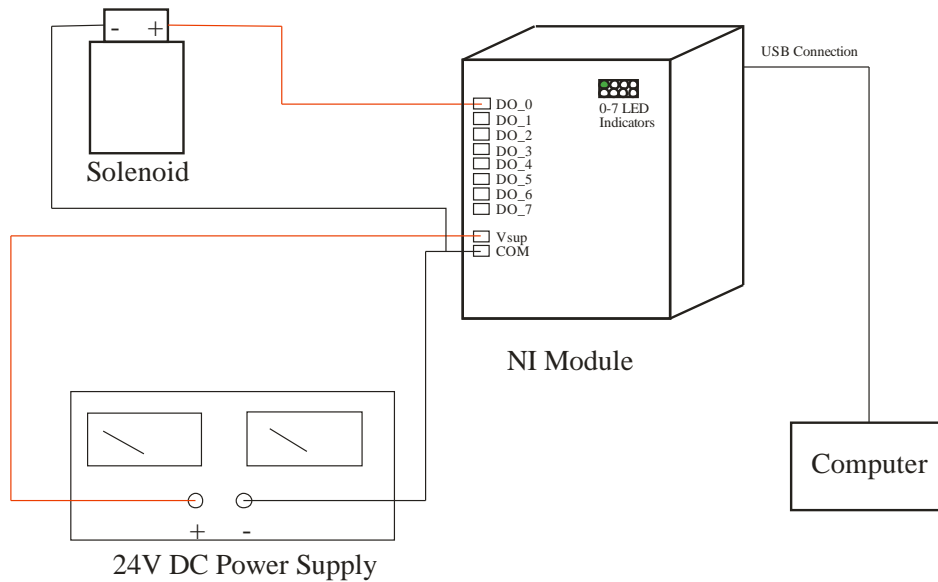


Figure 9: Wiring diagram of air solenoid connection to NI module

The automation aspect of the pultrusion system was controlled through the use of a LabView virtual instruments (VI) program that was developed specifically for the system. LabView VI's are computer controlled interfaces with a series of variable and switch controls that are connected to the driving components of a system. When creating a VI in LabView, the system is built with a block diagram that is represented in the operating interface as buttons on the front panel display as shown in Figure 8. Continuity loops, safety stops, and output functions are coded through the construction of the block diagram as shown in Figure 10. To control the air solenoids in the proper sequence, a true/false matrix was used to turn the proper solenoids on (true) and off (false) as the program runs continuously. The sequence consisted of five segments that correlated to the square cycle motion of the pulling mechanism: clamping, pulling, releasing, return to origin, and rest. Speed of each segment could be varied through user input on the front panel.

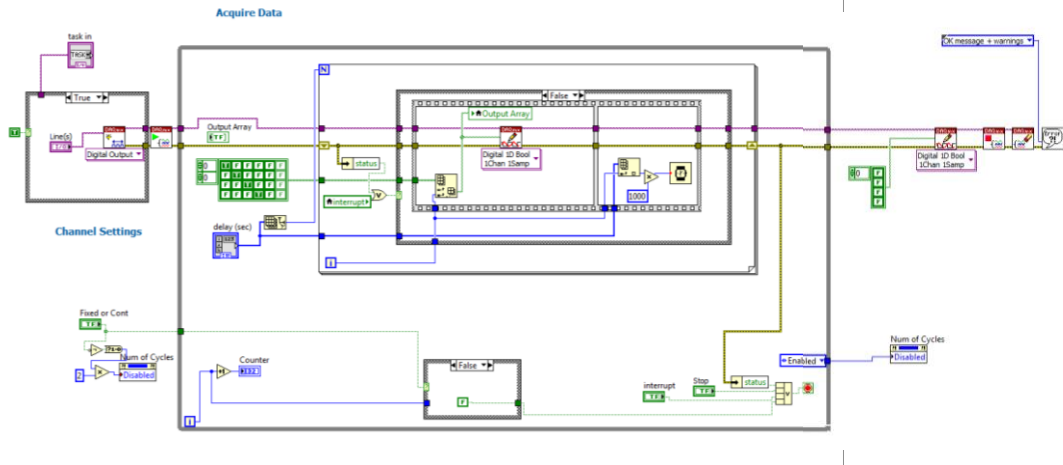


Figure 10: Block diagram of pultrusion VI

2.4 Press

The final station in the pultrusion system is the pneumatic press. The press serves to provide a uniform finish on the sample before it sets and to mold the wet sample into different shapes. The press consists of two pneumatic actuators mounted on a steel load frame. The actuators have a 2" stroke and are fitted with 8"x13"x1/2" heat treated aluminum plates connected to their pistons. The press is connected to the building air pressure and is controlled through a pressure regulator that maintains a constant pressure of 10-20 psi. Figure 11 shows the pneumatic press as it is about to press a sample.



Figure 11: Pneumatic press before pressing a plate sample

2.5 Sample Production

Through the use of the automated pultrusion system, several types of samples can be produced. The system allows for efficient manufacturing of TRC that produces consistent composite lamina. To adequately test the quality and versatility of the system, two types of samples were produced: plates and angled sections. Preparation for production includes the establishment of a workable mix design and the calculation of the required number of textile layers for the desired textile volume fraction. When casting samples, the VI controls the pulling mechanism which drives the production line. Manual tasks for manufacturing are simply laying and cutting of each coated textile upon the composite. Additional finishing of the matrix layers can be performed to improve final surface texture though pressing ensures a generally uniform and smooth composite surface.

2.5.1 Mix Design

For production of TRC samples, a general mix design was used in most following studies. A water to cement ratio of 0.32 and cement to sand ratio of 2:1 were used for all samples. 5% of the cement was substituted with silica fume and 10% was replaced with wollastonite for a total cement substitution of 15%. Superplasticizer was used to increase the workability of the mix, specifically for the paste bath to allow for better coating of the textile. Standard laboratory mixing procedures were followed as a fixed, 5L Hobart mixer was used to dry mix materials for one minute, followed by four minutes of wet mixing. Superplasticizer was added to the mix after two minutes of wet mixing. The mix proportions for all mixes are shown below in Table 1.

Table 1: Mix Design of TRC Samples

Material	Weight Percentage
Portland Cement (Type III/IV)	46.75%
Silica Fume	2.75%
Fine Silica Sand	27.5%
Water	17.5%
Wollastonite	5.5%
Superplasticizer	0.01%

2.5.2 Textile Volume Fraction

Before casting a TRC sample, the necessary number of textile layers must be calculated. The number of layers required is dependent upon sample thickness and the textile properties such as weave and diameter of fiber. A standard calculation was performed for every sample casting to ensure consistency between samples of different shape and volume. To calculate the necessary number of textile layers, the diameter of a fiber within the textile must be measured. With fibrillated fibers, the cross sectional area of each filament was multiplied times the number of filaments and resolved for the total fiber diameter. AR glass samples had a set diameter and could simply be measured with a pair of calipers. Next, the average number of yarns per unit length was measured. This was completed by counting the number of yarns across 3” in both the long and wide directions of the textile. These values were then divided by 3 to get the average value. The number per unit length values were multiplied by their respective dimensions and then summed and multiplied by the area of the fiber to get the total area of one textile layer. This volume was divided by the total volume of the sample to calculate the volume fraction of one

textile. The desired volume fraction was then divided by this value to get the total number of layers required.

2.5.3 Plate Production

Plate sections are the simplest samples to produce using the pultrusion system. After deciding on the desired textile volume fraction and batching the matrix, the system was prepared by filling the water and paste baths, greasing the pulling mechanism and rollers, and turning on the building air pressure. Also, textiles were placed on the roller and pulled through the system up to the pulling mechanism. Once the starting end reached the pulling mechanism, the system was able to run automatically. An initial layer of matrix was laid on a plastic-coated buffer board to act as the bottom laminate of the composite. The VI input delays were then set to control the speed of production. The system was then activated and the textile was pulled through the production line. As the coated textiles reached the press, they were laid upon the initial matrix layer. Textiles were continuously placed until the desired volume fraction was reached. Matrix was continuously added between the textile layers to ensure proper impregnation and even laminae. Once a sample was completed, it was wrapped in plastic and then pressed for 24 hours at a pressure of 15 psi. The samples were then demolded and moist cured for 28 days. Multiple plates can be cast and pressed simultaneously as shown in Figure 12 (a) and (b).

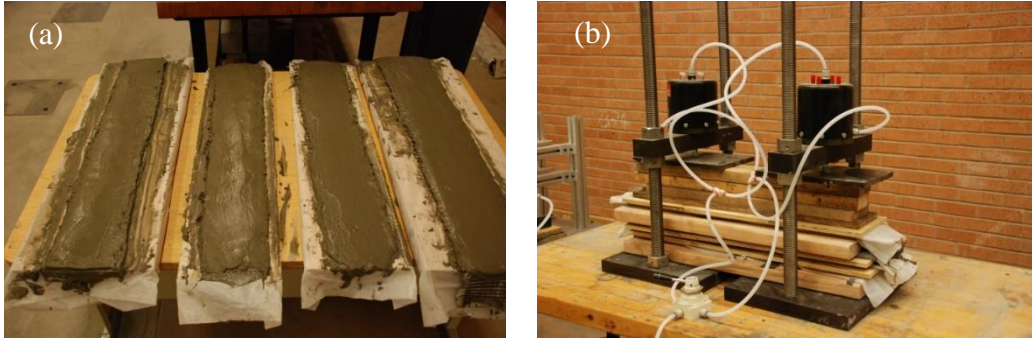


Figure 12: (a) Multiple plate samples cast in one session; (b) Pressing of multiple plates

2.5.4 Structural Shapes



Figure 13: Cross section of pultruded TRC angle

When casting structural shapes, such as the angle shown in Figure 13. with the automated pultrusion system, the procedure was similar to that used when casting plates. The matrix was batched and mixed using standard mixing protocol with a portion used for the top and bottom matrix layers and finishing and the rest used in the paste bath for coating textile. The system can operate with the same VI inputs and run continuously at the same speed. Matrix coated textiles were laid layer by layer as a flat plate with matrix added

between series of textile layers to ensure adequate thickness and volume fractions. The difference in casting was seen in the pressing and shaping of the sample. Once all layers were placed and hand finishing was complete, the flat plate was pressed at 10 psi with the pneumatic press to improve textile impregnation. After approximately 10 minutes, the press was raised and the sample was then shaped. This was completed through the use of the molds which helped to disperse the matrix paste and shape the composite. The wet sample was wrapped in plastic cloth and laid on the mold. As shown in Figure 3.4(b), buffer boards were used to ensure contact between the mold plates and the pneumatic press. The pneumatic press was turned on up to a maximum pressure of 20 psi which created a generally uniform, smooth surface structural shape. When casting angle sections, a series of steel angles can be used to create several structural sections during one casting. Figure 14 (a) and (b) shows the mold setup used for casting angle sections. Channels can also be produced using a similar technique with an outer jig made of two angles connected to cement board and a wooden board as the inner mold.

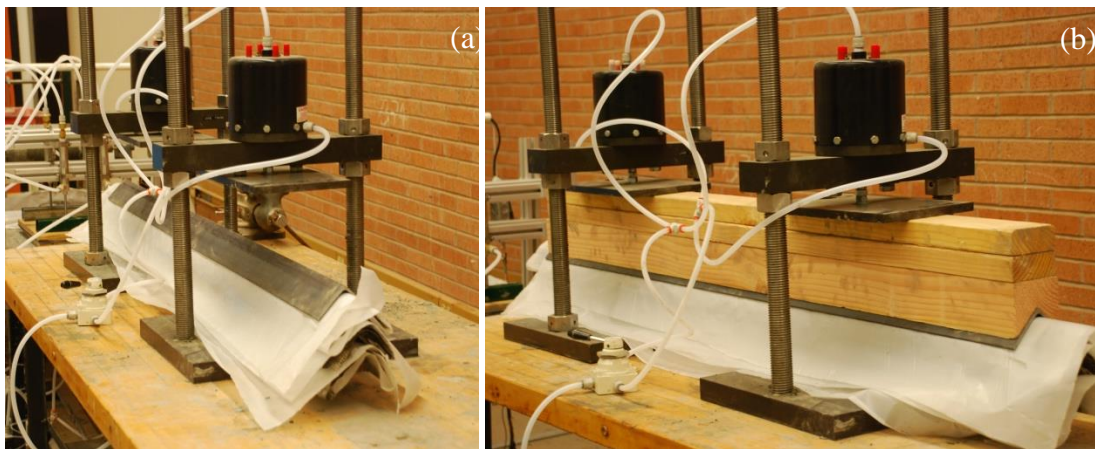


Figure 14: (a) stack of steel and TRC angles before pressing; (b) pressing of TRC angles

2.6 Testing Methods

To verify the strength of this composite production technique, testing of the pultruded samples must be performed. Textile within cementitious composites contributes to increased tensile strength and ductility, therefore static tension tests are the strongest method for studying the effect of the textile reinforcement on the composite. To properly test the range of produced samples, a series of tension tests for plates and preliminary tension and compression tests for angled sections were run at the Arizona State University Structures Lab. The compression testing of the angled section helps to show how the strength of the composite changes due to the length of the sample, similar to testing that would be run on a steel angle. The next three sections discuss the setup and results from the tension and compression testing of pultruded TRC sections.

2.6.1 Tension

When conducting tension tests on pultruded samples, a closed loop servo controlled test system was utilized. Using an Instron 55 kip capacity hydraulic load frame, samples were fixed at the top and bottom ends and pulled at a displacement rate of 0.05 in/min until reaching 0.05 inches when the displacement rate increased to 0.1 in/min and remained constant until failure. The test frame is controlled through MTS Station Manager Software with displacement of the bottom actuator used as the feedback signal.

2.6.2 Tension in Plates

From the large cast plates, the first two samples were cut using a wet diamond-blade tile saw into testing coupons of the dimensions of 12"x2.25"x0.5". Using a set of hydraulic grips, the specimens were gripped 2 inches from the bottom and top leaving a gage length

of 8 inches for the 4% samples and 6.5 inches for the 8% sample. The specimens were tested using the procedure from the previous section with an linear variable differential transducer (LVDT) mounted on each side of the specimens to better measure the elastic range of the stress-strain response. The LVDTs had a gage length of 3.5 inches and a range of approximately 0.33 inch. The test setup is shown above in Figure 15.

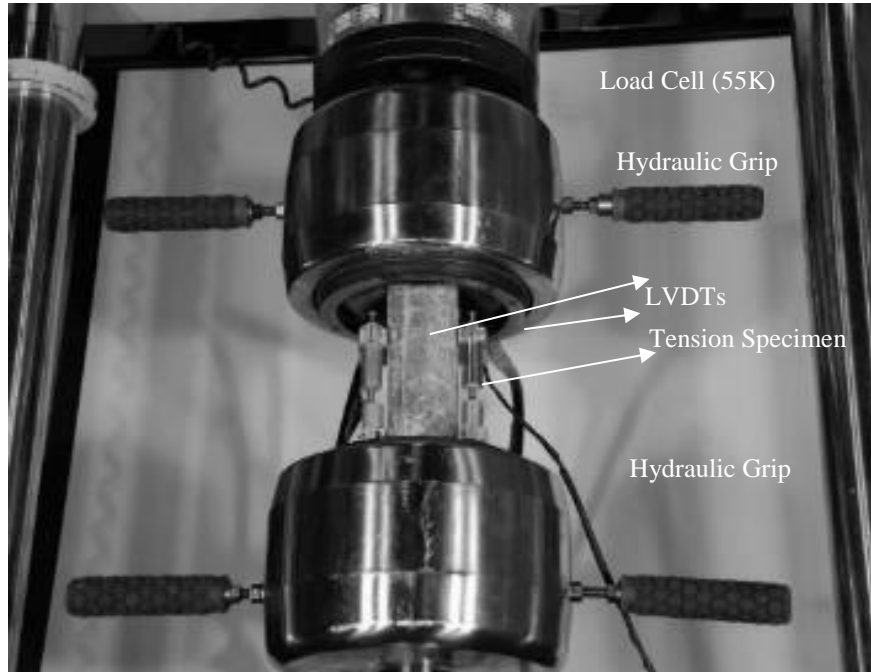


Figure 15: Tensile testing setup of TRC plate section

2.6.3 Tension in Angle Sections

When conducting tension tests in structural shapes, the gripping mechanism can become problematic. Gripping should be as analogous to real world connections as possible while remaining rigid to ensure proper testing. Bolt connections were used to grip concrete angles for tension trials. These bolts simulate connections in a large scale structure and can

lead to an adequate response. Special fixtures were made to create a rigid connection between the sample and the actuators of Instron load frame. Three different gripping systems were developed in the study explained in Chapter 5 of this report. The first testing setup is shown in Figure 16.



Figure 16: Tension testing setup of TRC angle on Instron load frame

3. COMPARATIVE ASSESSMENT OF UNIDIRECTIONAL FILAMENT WOUND FIBER REINFORCED CONCRETE VERSUS PULTRUDED TEXTILE REINFORCED CONCRETE

3.1 Overview

Through the use of the automated pultrusion system, several types of TRC systems can be manufactured efficiently and with adequate precision and quality control. Preparation for production includes the establishment of a workable mix design and the calculation of the required number of textile layers for the desired textile volume fraction. Manual tasks for manufacturing these systems include handling of the textile layers before and after the pultrusion process, stacking of the layers of textile and finishing of the matrix layers to ensure a smooth surface finish. The desired cross section is achieved through post manufacturing shaping by use of a die mold controlled by the in-situ pneumatic press as shown in the previous section. Through this process, many versatile system geometries of full scale length can be efficiently produced.

3.2 Experimental Program

An extensive experimental program was undertaken to evaluate the performance of unidirectional composite laminates with the mono filament MAC 2200 CB and multi filament MF 40 fibers at three different volume fractions ranging from 1-4%, and four different matrix compositions. The aging effect of these composites was studied for select specimens at 7 and 28 day curing periods. A total of three different mixes developed in this

study are summarized in Table 3. Direct tension tests and four-point bending tests performed on at least four replicate samples were tested for each mix design. A control mortar mix design was adopted with fly ash partial substitution of 15% of cement, sand/cement ratio of 0.45, and a water/binder ratio of 0.35. Mix design for this study is shown in Table 2.

Table 2: Mix design for polypropylene TRC study

Material	Weight Fraction (g/kg)	Weight Fraction (%)
Portland Cement (Type III/IV), C	450	45%
Fly Ash (Class F), FA	70	7%
Fine Silica Sand, S	230	23%
Water, W	180	18%
Wollastonite (NYAD-G), Wol.	45	4.5%

Fabrics are frequently made from single or multifilament yarns and the potential penetrability of the cement into the bundle spaces depends on the structure and the density of the weave. For example, the tightening of the joints that connect the weft and fill yarns induced by the junction points of the fabric strongly hold the filaments of the bundle and prevents them from being opened. Paste penetration into multifilament yarns leads to improve strength. This form of textile reinforced system (TRC) could be easily adopted and modified to fabricate different structural shapes such as channels, angles, hollow sections and rectangular plates of any desired length and cross-sections.

In the current study, MF-40 microfibers have been woven into textile form in plain and tricot weave patterns at RWTH Aachen University as shown in Figure 17. Open weave

is a basic one-face warp in which a knit is worked from one fully threaded warp. In the first row the thread forms a stitch on the first needle; in the second row this occurs on the third needle. Stitches are made alternately, first on one side, then on the other. In tricot weaves one thread forms stitches alternately in two neighboring columns. By the pulling of loops, stitches are made alternately on one side, then on the other [40].

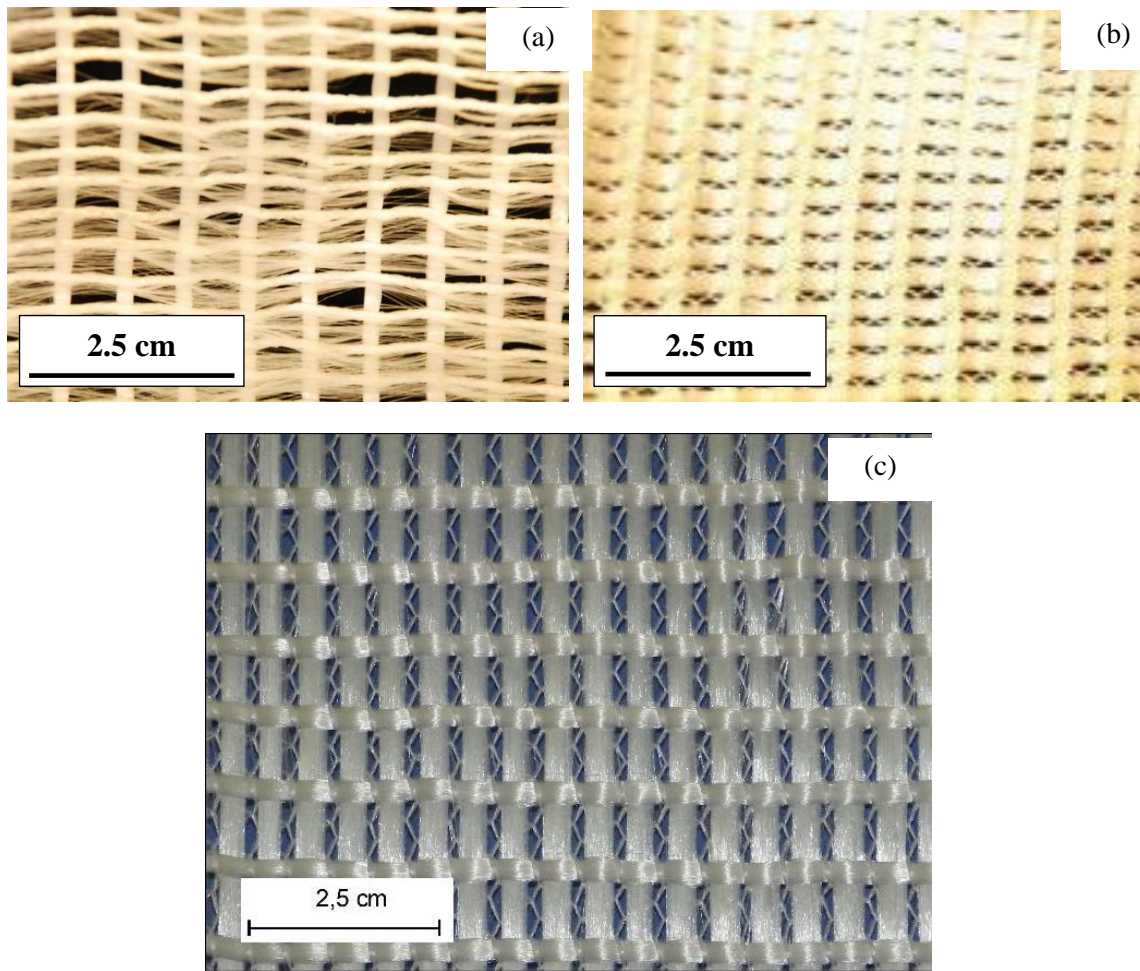


Figure 17: (a) Open weave patterns (b) & (c) tricot weave patterns of textiles woven from MF40 microfibers

TRC composites were tested under direct tension and flexure under static loading to characterize the strength, strain capacity, stiffness, and distributed cracking mechanisms. Mechanical properties of the newly developed textile reinforced composites (TRC) were compared to the filament wound continuous fiber composites studied earlier as identical dosages and mixture composition. Three distinct measures of damage under tensile loading include: quantitative crack spacing, stiffness degradation, and microstructural evaluation by optical microscopy will be evaluated. The three different TRC specimen groups studied are shown in Table 3.

Table 3: Groups of specimens of TRC developed in the study

Group ID	Yarn Type	Textile Weave	Yarn V_f (%)
I	PP	Open	4.0
II	PP	Tricot	4.0
III	PP	Open	8.0

Three sets of TRC laminate sections (30x6x0.5 in) were cast in the preliminary study of the textile materials with the two different weave patterns mentioned above. Direct tension tests were conducted on TRC coupons (12x2.25x0.5) after 7 and 28 days of curing. These trends are shown in Figure 20, wherein stress-strain responses of the TRC composites were compared to the continuous composites with continuous yarns of MF 40 after 28 days of curing. The composites were made with volume fractions of 4% and 8%.

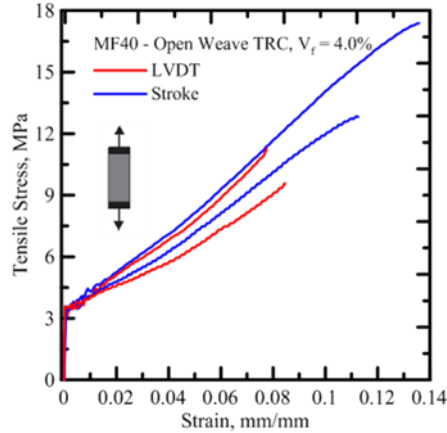


Figure 18: Comparison of LVDT and stroke response of 4.0% open weave TRC specimens

As evident the 28-day tensile strength of continuous composites with MF 40 fibers at 4% are considerable higher by 50 %, when compared to trends from the TRC composites with 4% textile dosage. It is to be noted that due to the two-dimensional structure of the woven textiles, effective vol. fraction of TRC composites along the loading direction is only 2%. Hence when the results from TRC with 8% of textiles is compared to the continuous MF 40 fibers at 4%, the tensile response is quite similar. Interestingly, the total strain capacity of the TRC composites is much higher compared to the continuous composites. This could be attributed to the tightening and interlocking effect of the woven filaments contributing to better ductility as opposed to continuous fiber reinforced composites. Table 4 shows the tension results from 4% open weave textiles.

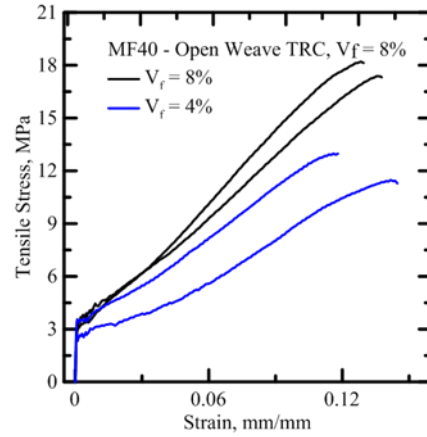


Figure 19: Comparison between 4% and 8% open weave TRC composites

Table 4: Tension results from open weave 4% polypropylene study

Replicate ID	Stress at BOP	Strain at BOP	UTS	Strain at UTS	Young's Modulus (LVDT)	Post-BOP Modulus	Post-FC Modulus	Work-Fracture (Stroke)
	MPa	mm/mm	MPa	mm/mm	MPa	MPa	MPa	N.mm
OW 4% #4	3.053	0.00015	13.000	0.189	19000	5000	120	110500
OW 4% #5	0.839	0.00006	9.443	0.220	9400	2500	110	76360
OW 4% #6	2.050	0.00007	11.503	0.227	28000	25000	110	123100
Avg	1.981	0.00009	11.315	0.212	18800	10833	113	103320
S.D	1.109	0.00005	1.786	0.020	9302	12332	5.7735	24183

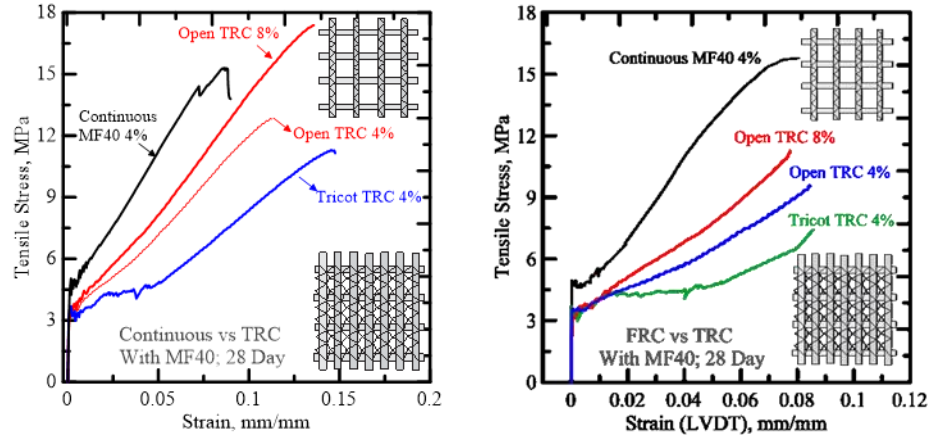


Figure 20: Stress-strain response of TRC with MF 40 textiles after 28 days of curing in tension

Flexural texting was also conducted on the micro fiber PP composites. The flexural responses versus that of continuous reinforced composites is shown in Figure 21 (a) with the tensile and flexural responses compared in Figure 21 (b). The tricot weave TRC composite showed a slightly better response than that of the open weave. This is likely due to additional stitching within the tricot textile which provides for a slight increase in ductility. The high volume fraction open weave TRC composite showed a response greater than that of the continuous MF40 specimen. This was likely due to the higher effective volume fraction in the continuous direction as well as toughening from the lateral fibers within the TRC composite. The trends show that the high volume TRC has a tensile strength lower than that of a continuous fiber composite with the same effective fiber volume fraction as well as a higher flexural response than that of a continuous fiber composite with a lower effective volume fraction.

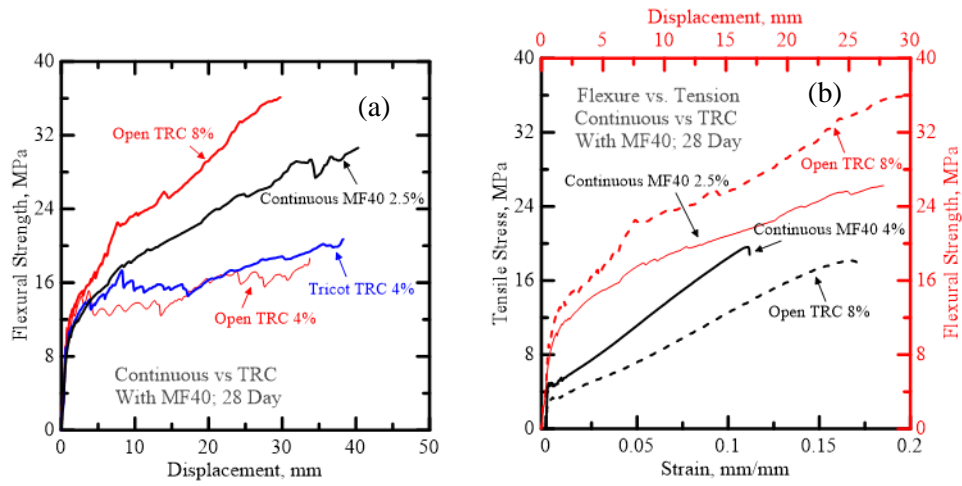


Figure 21: (a) Flexural response of MF40 TRC composites; (b) tensile versus flexural response

4. MECHANICAL PROPERTIES AND BEHAVIORS OF TEXTILE REINFORCED CONCRETE STRUCTURAL SHAPES

4.1 Overview

The objective of this study was to utilize the automated pultrusion system for continuous production of structural shapes using TRC materials with features for full scale industrial manufacturing. The equipment was used to produce TRC plate, angle, and channel sections using various types of woven polypropylene, carbon, and bonded alkali resistant (AR) glass meshes. Pultruded plates, angles and channels were tested in direct tension and compression to study crack formation and mechanical response. The strain field and distribution of cracking were monitored and verified using digital image correlation technique.

4.2 Sample Preparation

4.2.1 Matrix Phase

The automated pultrusion system was used to manufacture several types of samples with a consistent composite lamina. Two types of samples were produced: flat plates and structural sections. Flat plates were of the dimension of 1500 x 280x12 mm³ which were cut into smaller coupons of the dimension 300x64x12 mm³ and used primarily for testing unidirectional properties. Angles/Channels were of dimension L76x76x20 mm and C20x76x20 mm with lengths varying between 0.3 m to 1.2 m.

Preparation process required a workable mix design that was optimized with proportions of 1:0.32:0.5:0.1:0.05 representing the cementitious solids, water, sand,

wollastonite, and fly ash respectively. Superplasticizer was used to increase the workability of the mix in the paste bath to allow for better coating of the textile. Standard laboratory mixing procedures were done in a 5L Hobart mixer to dry mix materials for one minute, followed by four minutes of wet mixing. Superplasticizer was added to the mix after two minutes of wet mixing. The mix proportions for all mixes of 1% textile volume fraction are shown below in Table 5.

Table 5: Weight fractions per 1 kg of matrix mixture

Portland Cement (g/kg)	Fly Ash (g/kg)	Sand (g/kg)	Water (g/kg)	Wollastonite (g/kg)
467.5	27.5	275	175	55

4.2.2 Textile Components

Calculation of the required number of textile layers for the desired textile volume fraction was done with respect to sample thickness, weave density, number and diameter of filaments. A standard calculation was performed for every sample casting to ensure consistency among samples of different shape and volume. The percent difference between the desired textile volume fraction and the final specimen textile volume fraction was found to consistently be about 15%. This difference was caused by the inclusion of additional matrix paste in batching for allowance of adequate casting. The additional matrix used in casting was 15% throughout the entire study which is in-line with the volume fraction fluctuation. Regardless of paste changes, each TRC composite type was used with the calculated number of layers respective to the textile used so as to maintain uniformity between samples. The calculation of textile volume fraction was found through the equations and model shown in Figure 22.

$$V_{composite} = bht$$

$$A_{filament} = \left(\frac{D_{filament}}{2} \right)^2 \pi$$

$$A_{yarn} = A_{filament} n_{filament}$$

$$D_{yarn} = 2 \sqrt{\frac{A_{yarn}}{\pi}}$$

$$V_{textile} = \left((n_x b) h + (n_y h) b \right) A_{yarn}$$

$$v_f = \frac{V_{textile}}{V_{composite}}$$

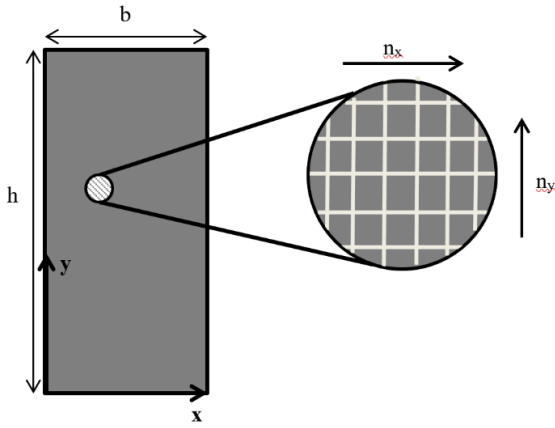


Figure 22: Textile volume fraction analysis

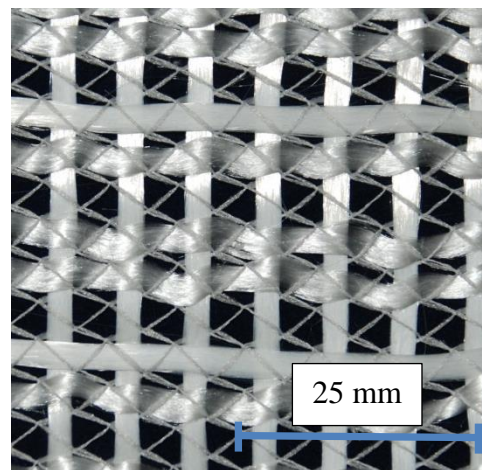
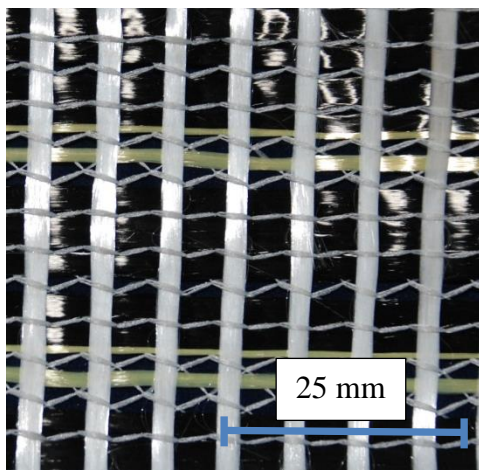
Where A_{xx} represents the cross sectional area of xx , D_{xx} represents the diameter of xx , V_{xx} represents the volume of xx , b is the composite width, h is the composite height, t is the composite thickness, $n_{filament}$ is the number of filaments in a yarn, n_x is the number of yarns per unit length along the x -axis (yarns oriented in the strong direction), n_y is the number of yarns per unit length along the y -axis (yarns oriented in the weak direction), and v_f is the volume fraction of reinforcement in the composite.

With fibrillated fiber textiles, such as the polypropylene and carbon tows used in meshes, the cross-sectional diameter of a single filament provided by the manufacturer was used to calculate the nominal diameter per unit length of textile. AR glass samples had a set diameter due to the protective coating of the filaments which was provided in the manufacturing details and was confirmed with a pair of calipers. Next, the average number of yarns per unit length was measured by finding the average number of yarns in the lateral and longitudinal direction. This was completed by counting the number of yarns across a square 76 mm sample in both the long and wide directions. The number of yarns in each

orientation was then divided by the relative length in each direction to find the number of yarns per mm. The number per unit length values were multiplied by the desired TRC sample dimensions and multiplied by the cross-sectional area of the yarn to find the total volume of yarn of one layer of textile. This textile volume was divided by the total volume of the TRC sample to calculate the volume fraction of the given textile. The desired specimen volume fraction was then divided by this value to get the total number of layers required within the TRC sample. Table 6 shows the reinforcement calculations for a standard TRC plate section of dimensions 13x279x1524 mm with each textile type. Figure 23 shows the carbon, polypropylene (PP) and alkali-resistant glass (ARG) textiles used in this study.

Table 6: Textile volume fraction for a typical TRC Plate sample (13x279x1524mm)

Textile	Filament Diameter (mm)	No. of Yarns	Area per yarn. (mm ²)	No. of Yarns per textile layer		Volume per textile layer (mm ³)	Volume Fraction per one layer (%)	Layers required for 1% v_f
				x-direction	y-direction			
ARG	0.0135	400	0.0573	111	609	19504	0.34	3
PP	0.04	100	0.1256	47	259	18193	0.34	3
Carbon	0.024	310	0.1402	55	304	23886	0.44	2



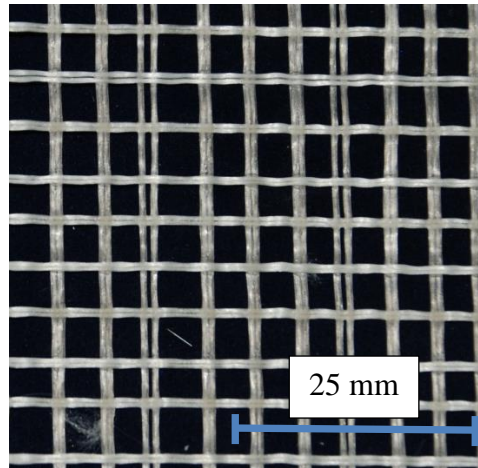


Figure 23: (a) Carbon, (b) PP, and (c) ARG textiles used to manufacture pultruded structural sections

4.3 Experimental Results

4.3.1 Mechanical Testing

Pultruded tension plates were cut into rectangular coupons with dimensions $12.7 \times 63.5 \times 305 \text{ mm}^3$ and tested in the Arizona State University Structures Lab. The coupons were pulled in direct tension using a closed loop servo controlled 245 kN capacity Instron load frame. Specimens were pulled at displacement rate of 1.27 mm/min with tests lasting about 2-3 minutes. Two 8.9 cm gage LVDTs were mounted to each side of the specimens to capture the stiffness degradation. The LVDTs were attached along the thinnest dimension to prevent crack bridging. Two static cameras were also used to capture images of the specimens for digital image correlation (DIC) which was used in the post-testing analysis as discussed later in this report. The setup of the tension tests is shown in Figure 24. Specimens were also tested in compression using this setup without the LVDTs.



Figure 24: Direct tension and compression testing setup for pultruded TRC coupons with digital image correlation

The mechanical response from the coupon testing is shown in Table 7. From the tension and compression testing, Carbon pultruded coupons were shown to have an ultimate tensile strength (UTS) of 12.5 MPa. PP coupons were shown to have an UTS of 8 MPa. ARG coupons were shown to have an UTS of 5.5 MPa. Specimens also exhibited distributed cracking across the gauge length during tension testing. The tension and compression replicate plots and failure patterns are shown in Figures 25-30. A comparison of all three textile composite types is shown in Figure 31.

4.3.2 Carbon Composites

Carbon coupons showed a tendency of a highly stiff elastic portion that was followed by a level yielding through the first 1% of strain and finally a post-crack strain hardening period that leads to failure. Figure 7 shows the tensile and compressive failure pattern observed in carbon specimens. Carbon pultruded TRC also exhibited extremely high strength and strain capacity with strength over twice that of ARG coupons and 50% higher than PP and a toughness of over triple that of PP and six times that of ARG. The compressive strength

was within 5% of the PP textile, but the carbon strength was ultimately lower due to the poor bonding of the carbon to cement from the tightness of the carbon weave that caused premature delamination than that of PP.

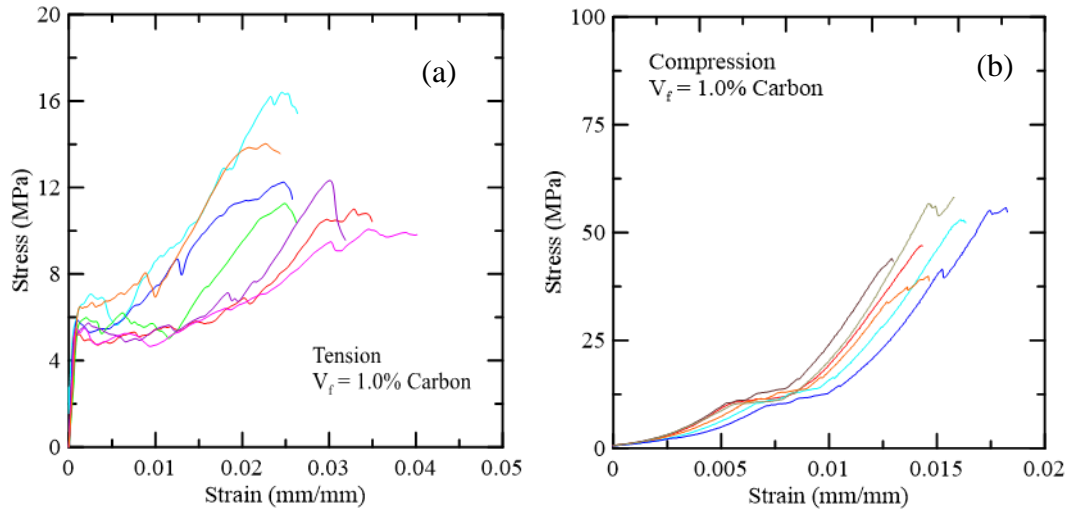


Figure 25: (a) Tension and (b) compression stress-strain response of carbon TRC specimens

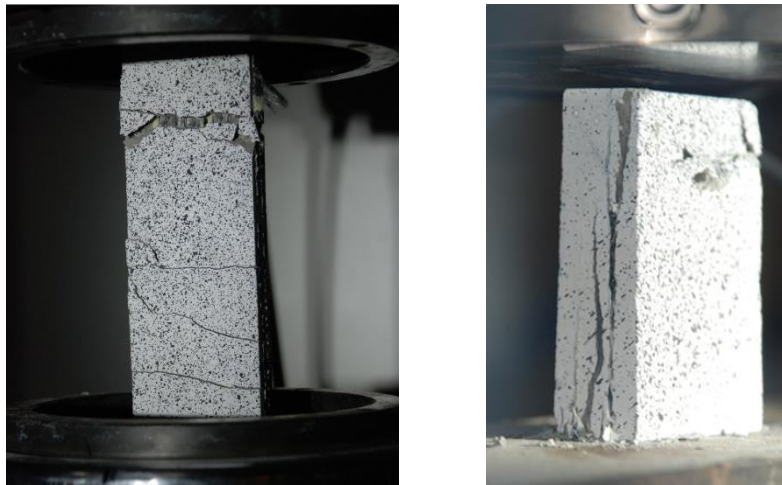


Figure 26: Tensile failure of carbon coupons displaying distributed cracking along length and compressive failure showing some delamination and local crushing

4.3.3 Polypropylene Composites

PP TRC coupons exhibited significant distributed cracking with small crack width along its gage length. It followed a two-phase mechanical response with a lower stiffness elastic portion than that of carbon and ARG TRC, and a linear strain hardening phase without any excessive nonlinear or constant yielding phase like that of ARG or carbon, respectively. Figure 9 shows the typical failure pattern of PP composite specimens under tension and compression. The compressive strength of the PP specimens was higher than that of carbon and ARG specimens due to better impregnation from the fibrillated mesh of the PP textile. The carbon mesh was tighter knit and led to earlier delamination than that of the open mesh PP textile.

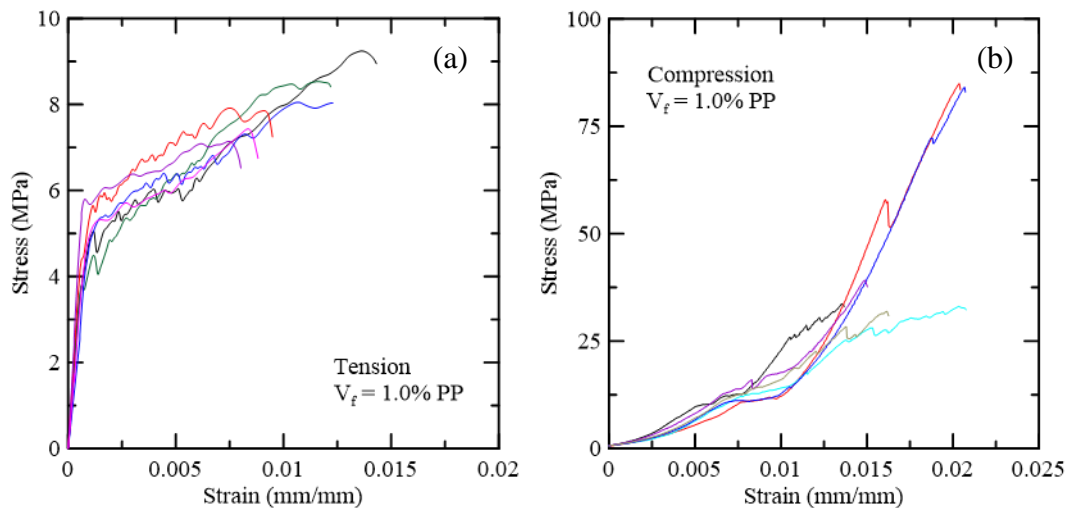


Figure 27: (a) Tension and (b) compression stress-strain response of PP TRC specimens

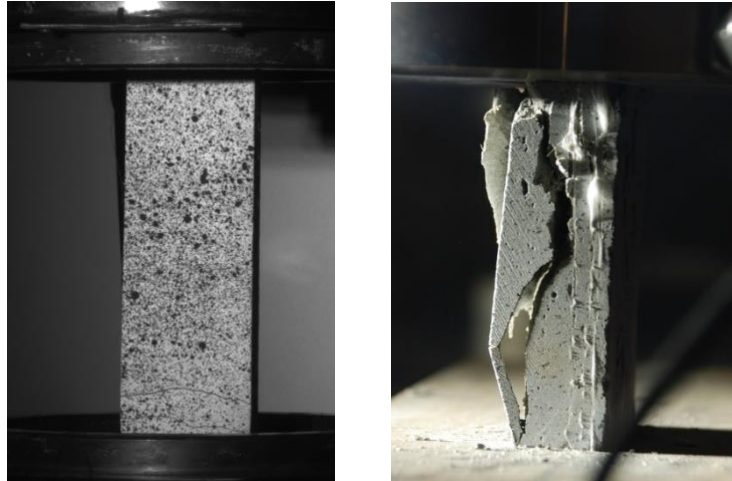


Figure 28: Tensile failure of PP composite showing extremely fine crack that eventually led to failure and compressive failure of PP specimen exhibiting buckling delamination

4.3.4 ARG Composites

ARG coupons had a more stiffened elastic response than that of PP specimens that was followed by a nonlinear yielding and strain-hardening phase with one or two large cracks forming, which is shown in Figure 10, as opposed to the multiple fine cracking seen in the other two composites. ARG coupons were the lowest strength and strain capacity composites. This was likely due to the low volume fraction of textile as TRC composites with high dosages of ARG textile tend to show significant strength with low strain capacity created by the stiffness from the glass reinforcement. The carbon and PP textiles were also fibrillated textiles which allowed for better paste to reinforcement bonding as opposed to the fine coated mesh of the ARG textile. The ARG textiles also showed significant delamination in compression testing, as shown in Figure 10, which was less dramatic in the other composites.

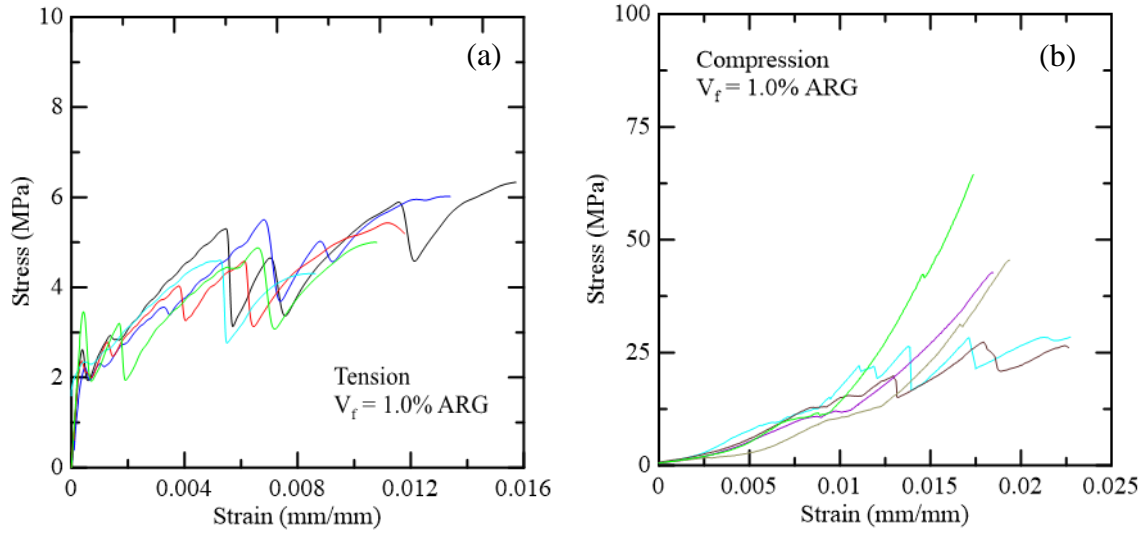


Figure 29: (a) Tension and (b) compression stress-strain response of ARG TRC specimens



Figure 30: Tensile failure of ARG coupon showing single large crack along gage length and failure in compression displaying splintering and excessive delamination between all textile layers

Table 7: Mechanical response properties of pultruded TRC coupons at 1% textile reinforcement

Textile	BOP Stress (MPa)	UTS (MPa)	Ultimate Strain (mm/mm)	Young's Modulus (E) (MPa)	Post Crack Modulus (E') (MPa)	Tensile Toughness (MPa)	Compressive Strength (MPa)	Compressive Modulus (E _c) (MPa)
Carbon	4.95	12.48	0.039	8114	306	0.302	49.70	3281

	0.58	2.13	0.009	1857	125	0.062	7.21	344
PP	4.29	8.05	0.015	6650	330	0.084	51.15	2897
	0.75	0.76	0.004	1765	79	0.022	25.99	1028
ARG	2.10	5.49	0.0174	7100	320	0.0594	42.28	3904
	0.52	0.72	0.0036	2563	135	0.0199	14.68	2350

****Average value, Standard Deviation**

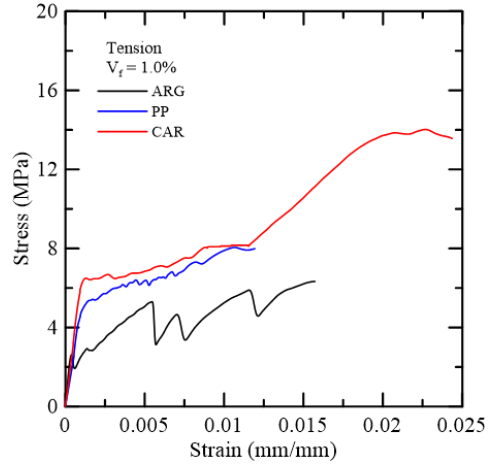


Figure 31: Comparative plot of ARG, PP, and Carbon TRC representative specimens

4.3.5 Structural Shapes



Figure 32: Pultruded TRC composite L and C structural sections

TRC structural sections can be cast uniformly to any length with the pultrusion system with minimal labor cost. Automated pultrusion manufacturing was used to develop large scale structural sections for full mechanical testing. As previously discussed, TRC plate sections were formed into angle and channel sections through use of mold fixtures. Upon curing, these structural sections were trimmed into clean and consistent sections as shown in Figure 32. These sections offer many economic and sustainable advantages such as durability, fire and water resistance, and low cost of production.

To assess strength of TRC structural sections and the effect of bolted connections, ARG tension coupons were also tested with both a fixed and bolted end connection. Coupons of dimensions $12.7 \times 63.5 \times 305 \text{ mm}^3$ were connected at one end with a single 8 mm bolt and pulled in tension. The other end was fixed in servo-hydraulic grips to mimic a fixed end connection while the bolt connection was connected as a pin to the other hydraulic grip. The bolted tension test setup and free body diagrams are shown in Figure 33.

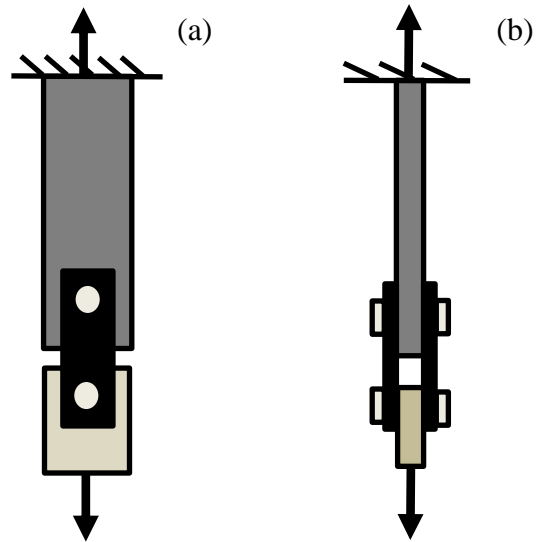


Figure 33: Single bolted tension test setup and (a) front facing free body diagram and (b) thickness profile free body diagram

The bolted coupons exhibited a lowered mechanical response as shown in Figure 34. The failure mode is also shown in Figure 14. The bolted specimens had an UTS of 4.47 MPa which showed a 19% reduction in strength from the direct tension ARG coupons. These coupon tests provided the baseline for multiple bolt connections as studied in full-scale structural shapes testing.

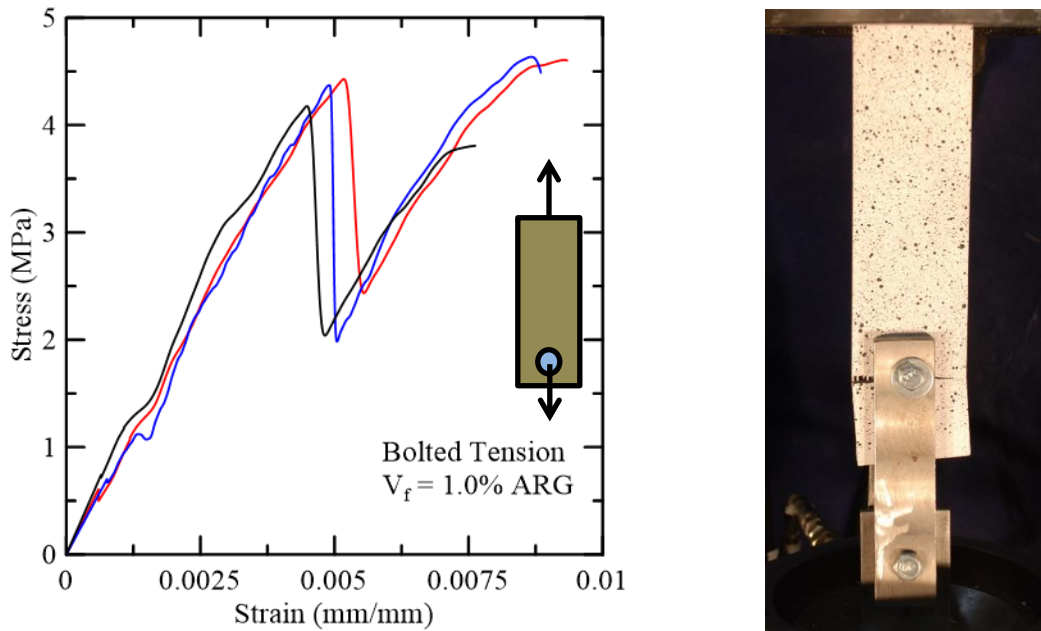


Figure 34: Stress strain response and typical failure mode of single bolted tension coupons

From the single bolted tension tests, ARG coupons were then tested with a two-bolt connection to study the expected behavior of full-scale structural shapes with bolted end connections. Coupons were connected at each end with an 8 mm bolt that was fed through a steel-to-wood angle tie that was attached to the actuator plate. The connections were

mirror to reduce the moment of the connection while still showing the shear eccentricity of the connection type. The test setup and free body diagrams are shown in Figure 35. Double bolted tensile strength was 2.9 MPa which showed a 47% strength reduction from direct tension testing. The stress strain response and failure mechanism for double bolted coupons are shown in Figure 36.

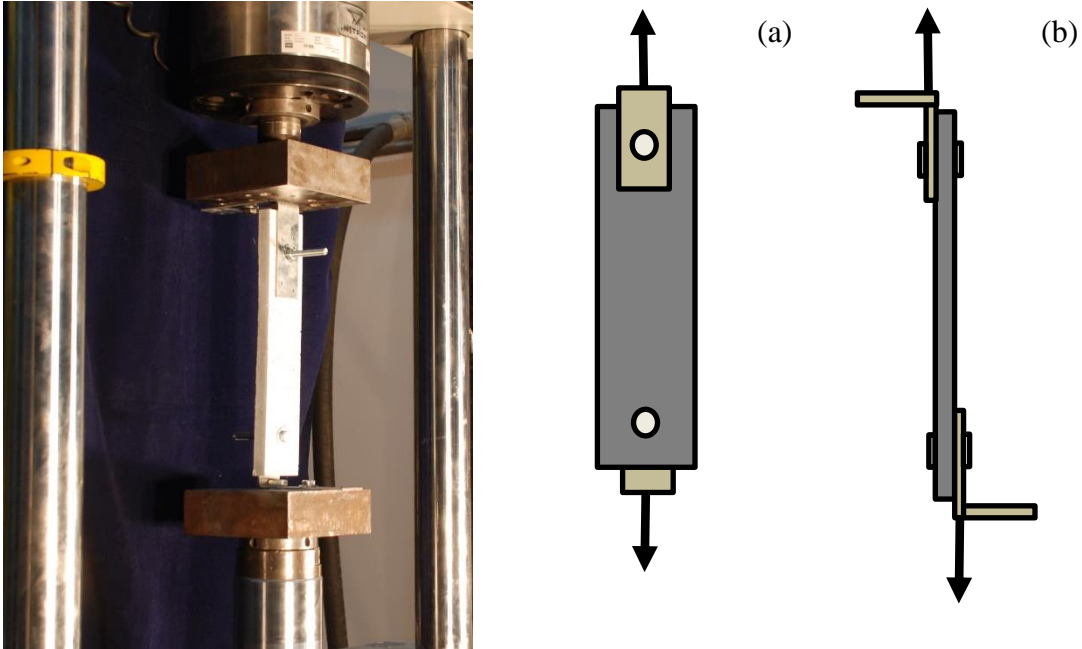


Figure 35: Double bolted tension test setup and (a) front facing free body diagram and (b) thickness profile free body diagram

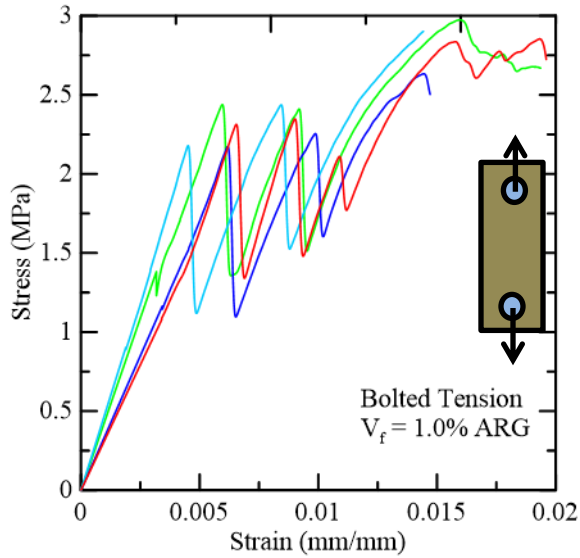


Figure 36: Replicate plot of ARG specimens tested in tension with bolted end connections

Several full-scale structural shape specimens were bolted to the Instron load frame used in the composite coupon testing. A mounted angle and channel section is shown in Figure 37. Angle sections were attached with six 8mm bolts per leg on each end. Channel sections were connected in the web with six 8mm bolts. The sections exhibited high ductility and toughness even with bolted connections which cause stress concentration and block shearing.



Figure 37: Tension test of full size TRC structural L-section and C-section with bolted connections on each leg

The comparative plot of direct tension, bolted tension, angle, and channel sections is shown in Figure 39. Angles exhibited distributed cracking with UTS of 2.7 MPa which was a 51% strength reduction from normal direct tension pultruded TRC coupons. Angle sections had stiffer connections with several bolts and failed most typically in tensile bearing failure at the bolts which is further confirmed in the angle UTS falling below the bolted tension strength of 4.5 MPa which was a 40% strength reduction. The mechanical response of TRC angles is shown in Figure 38. Channels were significantly weaker due to block shearing from eccentricity from the flanges not being restrained. The channels exhibited higher strain capacity but never exceed a strength of 2.0 MPa which illustrates a 64% reduction in strength from direct tension strength and a 55% reduction from bolted tension strength.

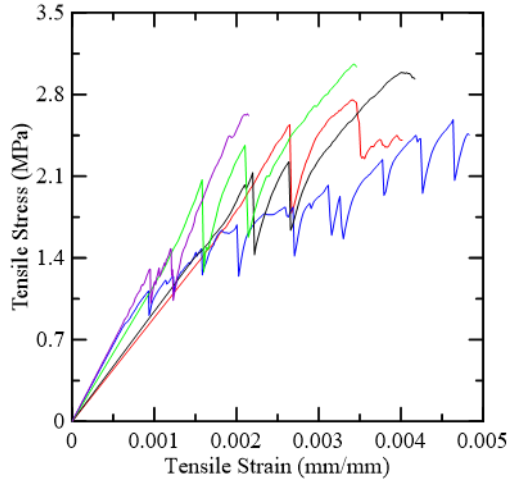


Figure 38: Tensile stress-strain replicate plot of TRC angles

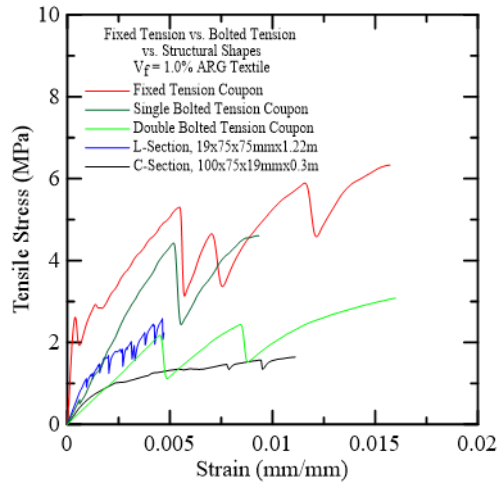


Figure 39: Comparative plot of ARG fixed and bolted coupons and structural shapes

5. EFFECTIVE OF CONNECTION TYPE FOR LARGE SCALE ARG TEXTILE
REINFORCED CONCRETE STRUCTURAL SHAPES

5.1 ARG Coupon Testing

Direct tension and compression testing was performed on pultruded TRC plate coupons that contained a 1% volume fraction of ARG textile reinforcement to gather the inherent material properties of the composite used for all structural shapes. The ARG textile used is highly flexible with openings that allow for adequate impregnation and moderate control of reinforcement volume. The mechanical properties are listed in Table 8 and the tension and compression stress strain replicate plots are shown below in Figure 40.

Table 8: Mechanical properties of TRC composites containing 1% ARG textile by volume

ARG TRC	BOP Stress (MPa)	UTS (MPa)	Ultimate Strain (mm/mm)	Young's Modulus (E) (Mpa)	Post Crack Modulus (E') (Mpa)	Toughness (Mpa)
AVG	2.10	5.49	0.0174	7100	320	0.0594
St. Dev.	0.52	0.72	0.0036	2563	135	0.0199

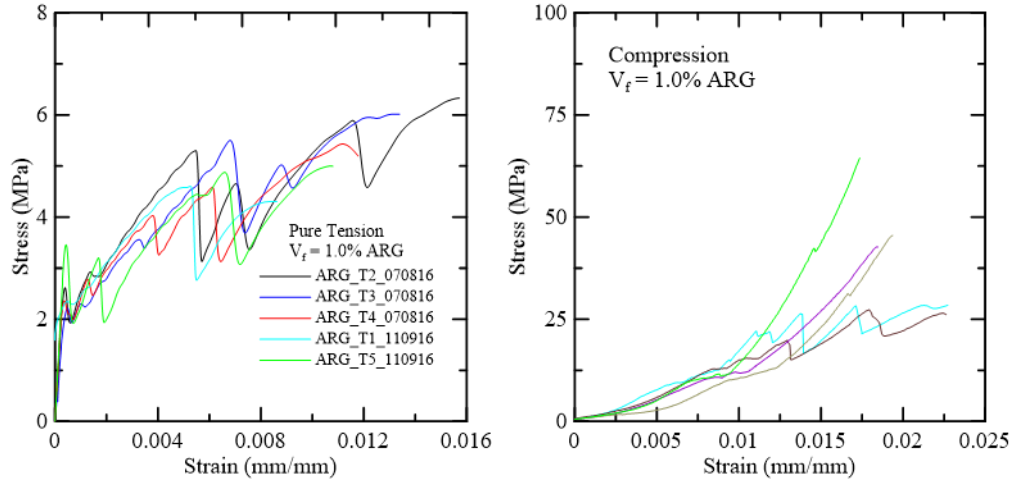


Figure 40: Tensile and compressive stress strain response of ARG plate coupons

5.2 Type I Gripping System – One bolt/vertical bolts

The first connection type (I) consisted of one 12 mm bolt per leg in a staggered form for tension and four 12 mm bolts that connect each leg of a TRC angle by passing through an aluminum block in a vertical, staggered orientation for compression. The aluminum block is connected to a steel plate attached to the load cell and actuator. Figure 40 shows a 20 x 76 x 76 mm³ TRC angle mounted on Type 1 gripping system. Shearing at the connections was the general mode of failure. The system was used to test angles in tension and compression. The schematic diagrams are shown in Table 14 in Appendix B. The mounted sample is shown in Figure 41.

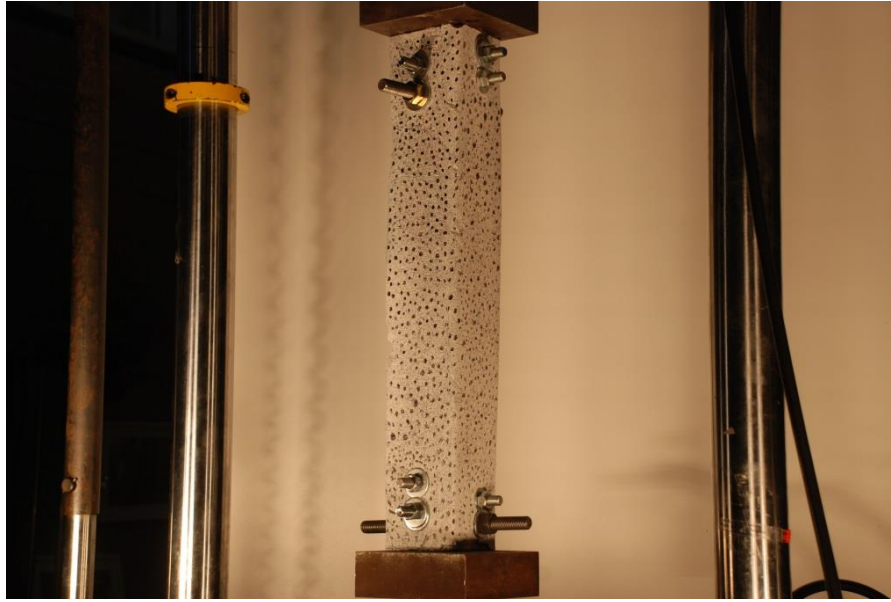


Figure 41: Compression specimen mounted on Instron frame with preliminary gripping system

Experimentation with this gripping system resulted in a bolt bearing failure at the bottom end in tension. It was concluded that Type I gripping system is not an ideal system to proceed with tension test though the result were fair enough.

5.3 Type II Gripping System – Two bolts per leg

Type II Gripping System used a similar setup to the previous grip in that an aluminum block connected to the actuator by a steel plate was used to connect to the sample. The sample was connected to the aluminum block with 10 mm bolts that were inserted into threaded holes in the aluminum block. A 12 mm aluminum block was used as a backer plate for each connected leg. This system was used to test both angles and channels for tension and compression. The system diagrams are shown in Table 15 in Appendix B. Failures of channels were most commonly shear block failures while angles failed with a tensile bearing failure. Stress strain response are shown in Figure 42 for Grip Type II.

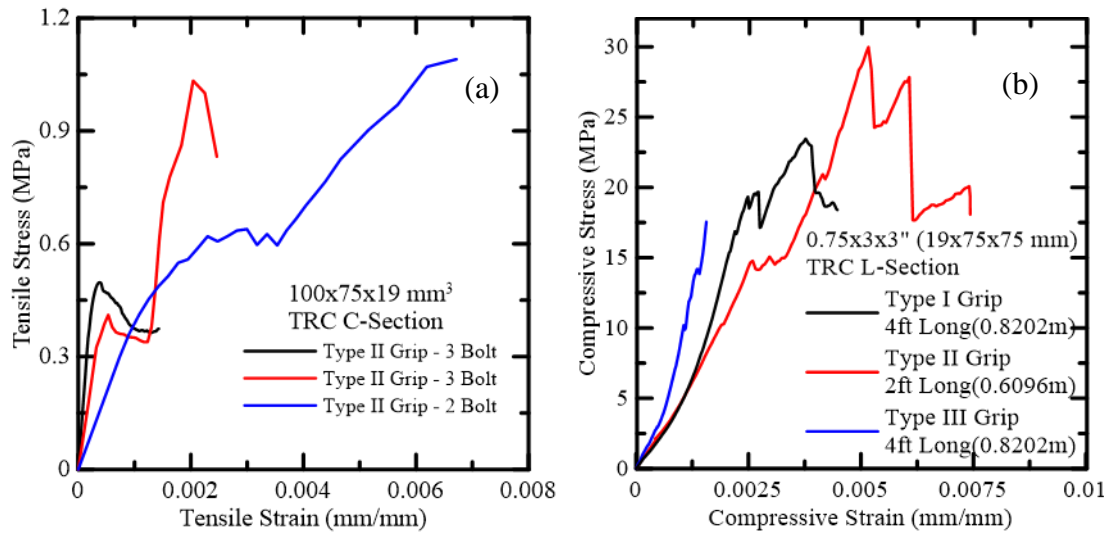


Figure 42: (a) Tensile Stress-Strain response of channels with Type II of 3 different configurations; (b) Compressive Stress Strain response of specimens connected with Type I, Type II, and Type III

Tensile stress strain responses of channels for all three configurations of Type II gripping system are shown in Figure 42 (a). Specimens typically reached two stages – Initial and Final crack. Until initial crack it has a stiff connection and undergoes no rotation. Initial crack is achieved between 0.35-0.6 MPa which is due to the orientation of grips and number of bolts considered for the connection. Red and black curves are of same configuration, Type II Grip – 3 Bolts, but their initial crack values vary due to the change in gauge length of sample considered for testing. The blue curve of Type II Grip – 2 Bolts showed a reduction on stiffness but a higher initial & final crack, and the specimen exhibits a higher strain capacity due to the improved connection. Maximum stress at which final crack achieved was of 1 MPa.

In Figure 42 (b), compressive stress strain response of angles tested with Type II Grip show a higher compressive strength and strain capacity over specimens tested with

Type I Grip. Compressive strength resulted due to Type II Grip was desirable. From both tensile and compressive stress strain curve tells that Type II gripping system displays improved mechanical response over Type I gripping system. The Type II Grip was further adapted and included in detailing of section behavior.

5.4 Type III Gripping System – Six bolts per leg

As the tensile strength of structures and parallel cracking of the structure was not achieved in previous grips, Type III gripping system was fabricated and assessed. Type III consisted of a set of Simpson Strong Tie angles that were bolted to the steel plate connected to the actuator. The sample was then bolted to each 6 x 38 x 100 mm³ tie with three 8 mm bolts spaced 25 mm apart. For channels, a 20 x 76 x 100 mm³ red oak board was used as a backer plate for each side of the specimen. For angles, due to the size limitations of the gripping configuration, a single oak backer board was used instead. Both specimen types saw tensile bearing failures as the typical failure modes. Grip diagrams for Type III grip is shown in Table 16.

As shown Figure 43 (a), tensile stress strain response of channels by Type III gripping system which resulted in a higher strength around 1.6 MPa. Whereas tensile stress strain response of angles, Figure 43 (b), resulted in lower strength with Type III (2.5 MPa) compared to Type II (3 MPa). However, specimens tested with Type III Grips showed a series of parallel cracks and tensile failure at 1/4 gauge length from the top connection which was never obtained in the previous grips. With increasing in number of bolts Type III gripping system of angles did not result in pure tensile failure at the bolted junction,

which was consistently seen in the previous grips Type I and Type II. In the case of channels tension failure occurred at the bolted connection but failure occurred throughout the entire cross section. All of these inferences conclude that Type III gripping system obtained significantly improved system mechanical response with typical failure mechanisms and modes of TRC composites exhibited by the test specimens. Specimen failure in tension and compression is shown in Figure 44.

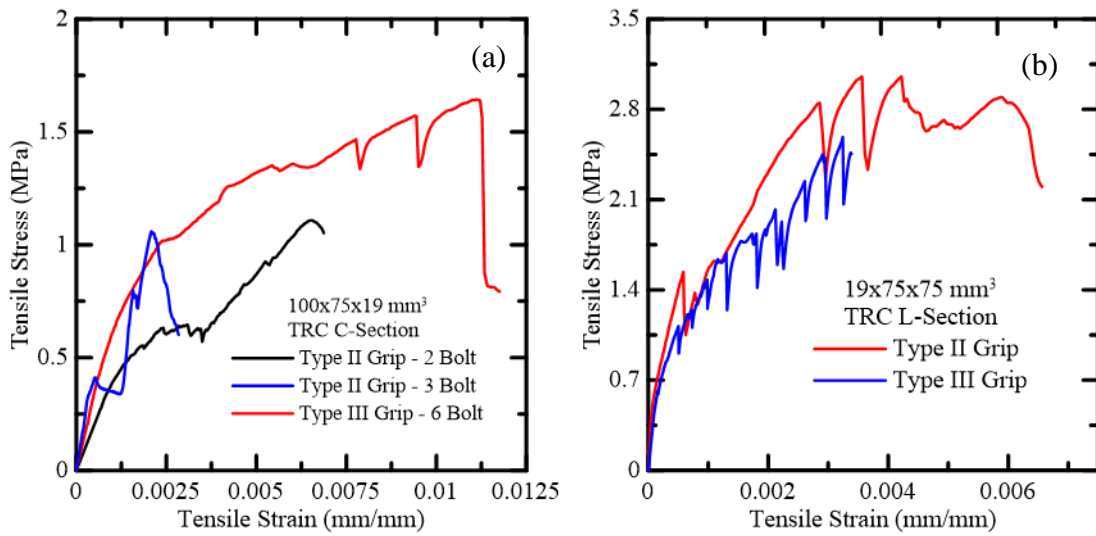


Figure 43: (a) Tensile Stress-Strain response of channels of Type II with 2 configurations and Type III gripping system (b) Tensile Stress- Strain response of angle of Type II and Type III gripping configuration.

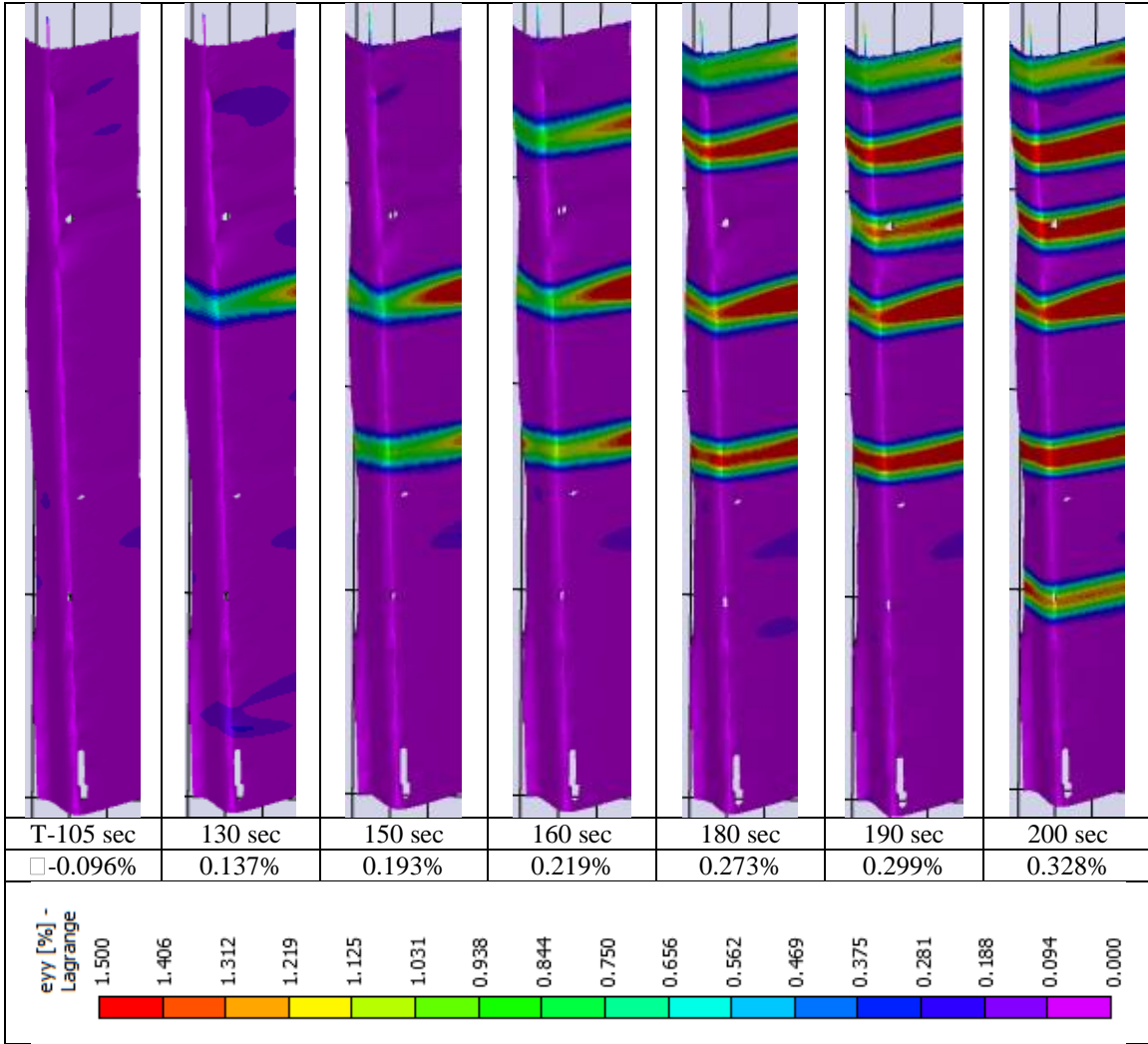


Figure 44: Tensile cracking and compressive buckling of 1.22 m long TRC L sections

5.5 Digital Image Correlation Analysis

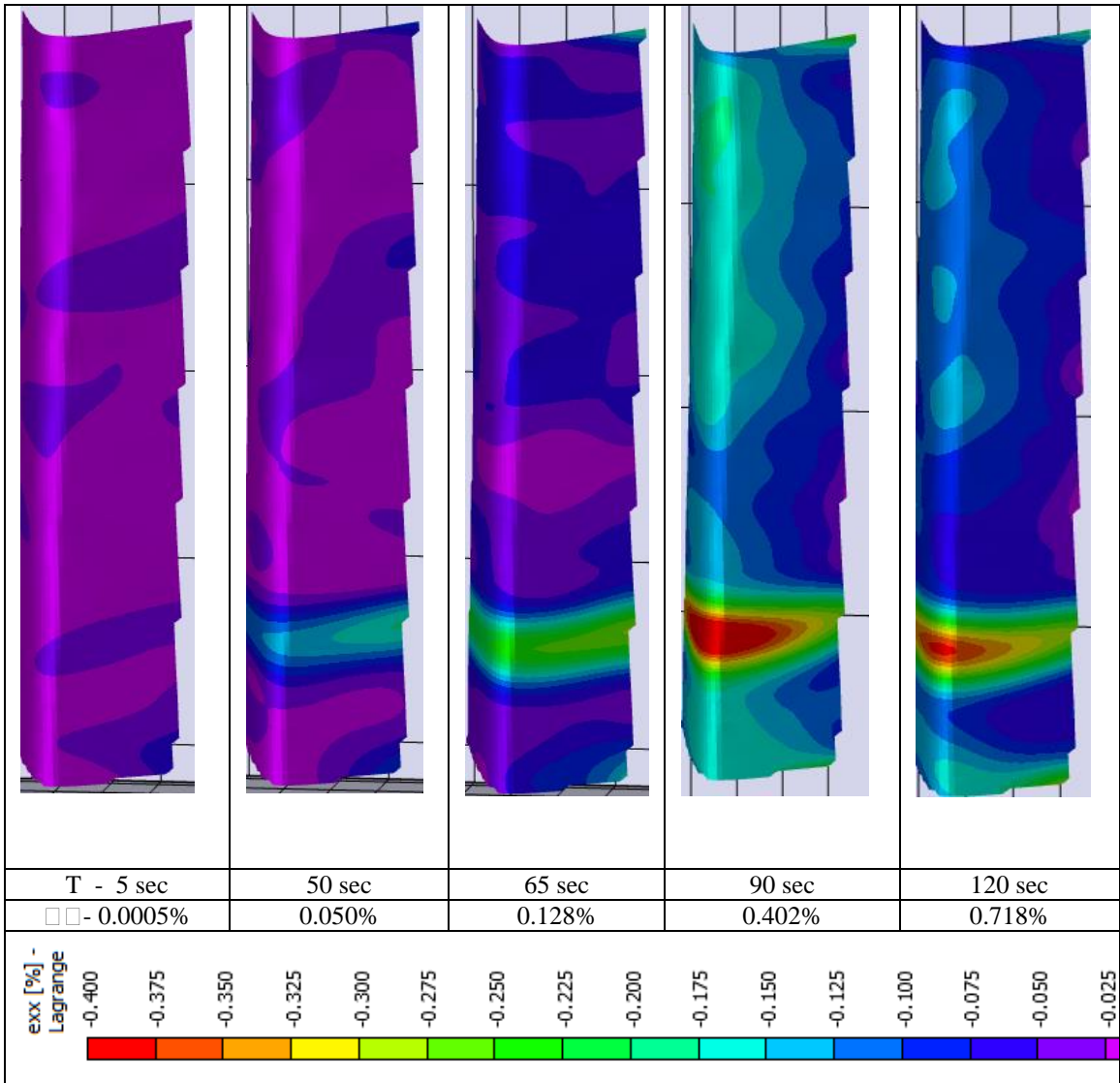
Full scale TRC angle sections tested in tension using Type III Grip exhibited the response shown above in Table 9. The specimen underwent parallel cracking with failure occurring within the gauge length. Image capture was restricted to approximately 3/4 of the gauge length due to specimen size and sensitivity of the camera. Cracking pattern and number were consistent between recorded response and image capture. As shown Table 9, the cracking pattern of the specimen trended similar to an expected tensile behavior response in which the load is further distributed across the sample after each crack attains the maximum yield strength of the particular portion. This process continues until ultimate system failure which supports the theory of stress distribution. Through DIC analysis, crack spacing, crack width, and stress analysis can be conducted to correlate results presented from the test actuator.

Table 9: Tension Test: 1.22m Test Type III Grips



The DIC analysis of a specimen tested in compression using Type II Grip is shown in Table 10. The specimen displayed buckling tendencies as seen in the increased lateral strain near the bottom end of the gauge length. Strain is concentrated more towards the spine of the angle as to be expected. At high global strain, lateral strain is mitigated more evenly across the sample.

Table 10: Compression Test: Type II Grip



6. CONCLUSION

6.1 Relevance

TRC is a strong and economic material that can be fashioned into a variety of structural shapes. These structural shapes hold much higher tensile capacity than traditional cement and as such can be used in small and large scale construction projects. The biggest limits for wide-scale use of TRC have been that the casting process is extremely time intensive and sensitive. Combined with a lower tensile strength than structural steel, TRC has seen a limited use in the construction industry. One of the ultimate benefits of the automated pultrusion system is that it provides for rapid and continuous production of TRC without the need of significant manual involvement. TRC sections are also more consistent as each section is pulled from the same production line with constant paste and textile supply and consistent pressing and finishing. Batch proportions are easier to control and textiles impregnate better within the composites due to the DC rollers and pneumatic pressing. With this streamlined and effective manufacturing technique, pultruded TRC can become a viable alternative to steel, wood, and aluminum.

6.2 Applications

As a construction material, pultruded TRC can be used for structural members undergoing compression, bending, and tensile loads that would typically cause plain concrete to fail. Despite high carbon emissions when producing cement, TRC is extremely sustainable due to the high resistance and durability of the material. It is fire and water proof and with proper expansion joints, durable to a wide range of temperatures. TRC sandwich panels can be efficiently produced with the pultrusion system. These panels

consist of an aerated concrete slab with a thin top and bottom layer of TRC as shown in Figure 45.



Figure 45: Pultruded TRC sandwich section

6.3 Future of study

With the pultrusion system successfully functioning, further assessment of properties and applications of structural shapes made of TRC is the primary focus of future studies. Due to the ease and consistency of manufacturing of these shapes, a large sample size of different TRC structural sections can be produced. Compression and tension tests will be run with the current testing fixtures to study effects such as volume fraction, textile type, shape geometry, etc. With a material database, the design of structures using TRC structural sections becomes feasible. Aggregate design strengths allow for computer design optimization of TRC structures that implement steel design principles. Both computer modeling and experimental construction will be necessary to complete this next phase of study. This thesis helps to verify TRC as a suitable and highly economical alternative to wood sections within structures.

7. REFERENCES

1. Mobasher, B., Peled, A., & Pahilajani, J. (2006). Distributed cracking and stiffness degradation in fabric-cement composites. *Materials and Structures*, Vol. 39, pp. 317-331.
2. Peled, A., Bentur, A., & Yankelevsky, D. (1999). Flexural performance of cementitious composites reinforced with woven fabrics. *ASCE Journal of Materials in Civil Engineering*, Vol. 11(4), pp. 325-330.
3. Peled, A., Cohen, Z., & Gries, T. (2008). Influences of textile characteristics on the tensile properties of warp knitted cement based composites. *Cement and Concrete Composites*, Vol. 30, pp. 174-183.
4. Sasi, E., & Peled, A. (2015). Three dimensional (3D) fabrics as reinforcements for cement based composites. *Composites: Part A*, Vol. 74, pp. 153-165.
5. Mobasher, B. Pivacek, A., and Haupt, G. J., Cement based cross-ply laminates, *Journal of Advanced Cement Based Materials*, No. 6, 1997, pp. 144-152.
6. Peled, A., Sueki, S., & Mobasher, B. (2006). Bonding in fabric–cement systems: Effects of fabrication methods. *Cement and Concrete Research*, Vol. 36(9), pp. 1661-1671.
7. Peled, A., & Mobasher, B. (2007). Tensile behavior of fabric cement-based composites: pultruded and cast. *ASCE Journal of Materials in Civil Engineering*, Vol. 19(4), pp. 340-348.
8. Soranakom, C., & Mobasher, B. (2009). Geometrical and mechanical aspects of fabric bonding and pullout in cement composites. *Materials and Structures*, Vol. 42, pp. 765-777.
9. Sueki, S., Soranakom, C., Mobasher, B., & Peled, A. (2007). Pullout-slip response of fabrics embedded in a cement paste matrix. *ASCE Journal of Materials in Civil Engineering*, Vol. 19(9), pp. 718-727.
10. Peled, A., & Mobasher, B. (2005). Pultruded fabric-cement composites. *ACI Materials Journal*, Vol. 102, No. 1, pp. 15-23.
11. Igarashi, S., Bentur, A., & Mindess, S. (1996). The effect of processing on the bond and interfaces in steel fiber reinforced cement composites. *Cement and Concrete Composites*, Vol. 18, pp. 313-322.
12. Goldsworthy, W. B. (1971). *U.S. Patent No. 3,556,888*. Washington, DC: U.S. Patent and Trademark Office.

13. Davies, L. W. (1994). *U.S. Patent No. 5,324,377*. Washington, DC: U.S. Patent and Trademark Office.
14. Ishida, H. (1994). *U.S. Patent No. 5,294,461*. Washington, DC: U.S. Patent and Trademark Office.
15. Peled, A., Mobasher, B., & Cohen, Z. (2009). Mechanical properties of hybrid fabrics in pultruded cement composites. *Cement and Concrete Composites*, Vol. 31 (9), pp. 647-657.
16. Devlin, B. J., Williams, M. D., Quinn, J. A., & Gibson, A. G. (1991). Pultrusion of unidirectional composites with thermoplastic matrices. *Composites Manufacturing*, Vol. 2(3-4), pp. 203-207.
17. Carlsson, A., & Åström, B. T. (1998). Experimental investigation of pultrusion of glass fibre reinforced polypropylene composites. *Composites Part A: Applied Science and Manufacturing*, Vol. 29(5), pp. 585-593.
18. (2010). Cold-formed steel in building construction. *Cold-Formed Steel Profile*. Washington, D.C.: Steel Market Development Institute.
19. (2000). *Light gauge steel construction: A completed study of the 2000 north American market*. Essex, CT: Ciprus Limited, LLC.
20. (2016). *Growth opportunities in the global roofing materials market*. Irving, TX: Lucintel.
21. Kovarik, S. (2009). *Why build with steel? Utilizing light gauge steel framing systems*. Warren, OH: Ron Blank & Associates.
22. Thompson, K. (2015). *2016 Economic outlook for cold-formed steel framing*. Falls Church, VA: Steel Framing Industry Association.
23. (2016). *Steel framing: A market on the move*. Harrison, OH: American Wall & Ceiling Institute.
24. (2014). *Composite wall testing of non-structural drywall studs for SFIA and SSMA*. Cambridge, ON, Canada: Structural Testing and Research Inc.
25. Serrette, R. (1997). New shear wall test data gives engineers additional design flexibility. *Newsletter for the Light Gauge Steel Engineers Association*. Seattle, WA: Light Gauge Steel Engineers Association.

26. Littlefaire, J. (2016). *2016 Top markets report building products and sustainable construction*. Washington, D.C.: US Department of Commerce.
27. (2016). *Growth opportunities in the global roofing materials market*. Irving, TX: Lucintel.
28. Werner, T. et al. (2010). Uses and desirable properties of wood in the 21st century. *Journal of Forestry*. West Lafayette, IN: US Forest Service.
29. Wegner, T. (2009). *Wood products research in the USA*. Madison, WI: US Forest Service.
30. Wallace, D. et al. Multi-story wood frame construction in the United States. *NZ Timber Design Journal*. Issue 2, Volume 7.
31. (2012). Multi-story wood construction. *Engineering News-Record*. Troy, MI: ENR.
32. Wegner, T. et al. (2005). *Nanotechnology opportunities in residential and commercial construction*. Madison, WI: US Forest Service.
33. Mobasher, B., Li, C.Y., Modeling of stiffness degradation of the interfacial zone during fiber debonding, *Composites Engineering* 5 (1995) 1349-1365.
34. Silva, F., Mobasher, B., Soranakom, C. and Toledo Filho, R., "Effect of Fiber Shape and Morphology on the Interface Mechanical Characteristics in Sisal Fiber Cement Based Composites," *Journal of Cement and Concrete Composites* Volume 33, Issue 8, September 2011, Pages 814-823
35. Silva, F., Butler, M., Mechtcherine, V., Zhu, D., Mobasher, B. Strain rate effect on the tensile behavior of textile-reinforced concrete under static and dynamic loading, *Materials Science and Engineering A*, 2011, 528, 1727-34.
36. Bauchmoyer, J. (2016). Development of an automated pultrusion system for manufacturing of textile reinforced cementitious composites. Barrett, the Honors College Thesis. Arizona State University, Tempe, AZ.
37. Dey, V., Kachala, R., Bonakdar, A., Mobasher, B., Mechanical properties of micro and sub-micron wollastonite fibers in cementitious composites, *Construction and Building Materials*, 2015, 82, pp. 351-359.
38. Kazuhisa, S., Noayoshi, K., Yasuo, K., "Development of carbon fiber reinforced cement", *Advanced Materials: The big Payoff National SAMPE Technical Conference*, Publ. by SAMPE, Covina, CA, USA, Vol. 21, 1998, pp. 789-802.

39. Nishigaki, T., Suzuki, K., Matuhashi, T., and Sasaki, H., "High strength continuous carbon fiber reinforced cement composite (CFRC)", Proceeding of the third international symposium on brittle matrix composites, Brandt, A. M. and Marshall, I H. (Eds.), Warsaw, Poland, Elsevier Applied Science, 1991, pp. 344-355.
40. Weblinks: <http://warpknits.vrtxinc.com/product/all-categories/tricot-knit-fabric>;
<http://www.norcostco.com/sharkstooth-scrimmaterial-20-flame-retardant-white.aspx>;
http://en.texsite.info/Tricot_weave

APPENDIX A

POLYPROPYLENE TRC TENSION DATA

Table 11: Analyzed tension test results from TRC specimens (average in bold, std. dev. in regular fonts)

Grp ID	Specimen Type	V _f	Age	Stress at BOP	Strain at BOP	Stress at First Crack	Strain at First Crack	UTS	Strain at UTS	Ult. Strain	E. Modulus	Post-BOP Modulus	Post-FC Modulus	Work - Fracture (Stroke)	Toughness at 2.5% strain	Toughness at 5% strain	Toughness at 10% strain
		%	Days	MPa	mm/mm	MPa	mm/mm	MPa	mm/mm	mm/mm	MPa	MPa	MPa	N.mm	MPa	MPa	MPa
1	Micro Fiber-Open Weave	4	7	1.769	0.0005	2.706	0.00010	11.22	0.181	0.203	14233	15500	96	100647	0.07	0.16	0.45
				0.146	0.0007	0.094	0.0007	0.96	0.005	0.015	5654	707	7	1649	0.00	0.01	0.04
1a	Micro Fiber - Open Weave	4	28	1.587	0.0006	2.443	0.00035	13.06	0.201	0.217	13500	9833	130	131557	0.06	0.16	0.45
				0.655	0.0001	0.983	0.00030	4.59	0.031	0.025	12946	13137	35	59865	0.03	0.08	0.25
3	Micro Fiber - Open Weave	8	30	2.449	0.00011	3.020	0.00048	17.62	0.176	0.182	25233	1633	197	187567	0.09	0.24	0.69
				0.158	0.0004	0.197	0.00013	0.53	0.009	0.013	16651	404	6	10650	0.01	0.02	0.04
4	Micro Fiber - Tricot Weave	4	8	1.994	0.0007	2.599	0.00021	10.46	0.235	0.240	20667	3267	100	135967	0.07	0.16	0.37
				0.218	0.0005	0.092	0.0009	0.57	0.013	0.010	9713	611	20	3037	0.00	0.01	0.01
4a	Micro Fiber - Tricot Weave	4	30	2.203	0.0006	3.439	0.00072	10.88	0.235	0.240	23000	725	90	153050	0.08	0.18	0.42
				1.003	0.0003	0.376	0.00095	0.64	0.003	0.000	16971	672	15	1909	0.00	0.01	0.01

Table 12: Analyzed flexural test results from TRC specimens (average in bold, std. dev. in regular fonts)

Group ID	Specimen Type	Stiffness	PEL Load	PEL Deflection	Cracking Load	Cracking Deflection	L/50			L/150			L/600			Flex. Strength	Defl. at Max Stress	Total Toughness
							Load	Residual Stress	Toughness	Load	Residual Stress	Toughness	Load	Residual Stress	Toughness			
							<i>N</i>	<i>MPa</i>	<i>N.mm</i>	<i>N</i>	<i>MPa</i>	<i>N.mm</i>	<i>N</i>	<i>MPa</i>	<i>N.mm</i>			
1	Micro Fiber - 4.0% - Open Textile	458	111	0.71	150	0.85	144	6.68	156	146	6.75	63	49	2.35	13	20	32.9	6772
		157	11	0.22	6	0.21	17	0.49	80	21	0.32	34	13	0.24	10	4	2.2	350
2	Micro Fiber - 4.0% - Tricot Textile	948	209	0.59	282	1.87	261	7.10	252	218	5.95	90	111	3.03	24	20	34.7	13653
		758	86	0.07	62	1.42	137	0.98	154	105	0.49	49	82	0.80	19	2	3.5	8467
3	Micro Fiber - 8.0% - Open Textile	1247	205	0.71	294	1.01	323	7.74	324	256	6.14	124	153	3.75	47	34	31.6	21081
		918	76	0.28	71	0.36	90	1.10	164	109	2.06	88	99	2.33	45	4	1.8	4806

APPENDIX B

TRC STRUCTURAL SHAPE GRIPPING FIXTURES

Table 13: Type I Grip Diagrams

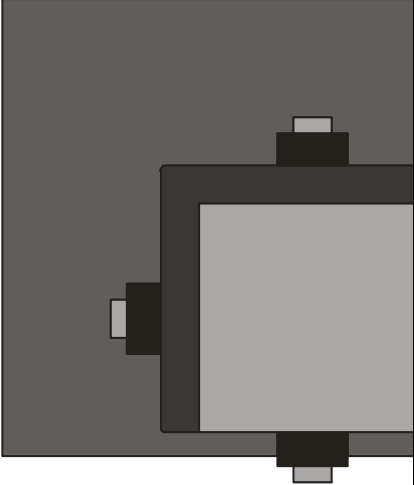
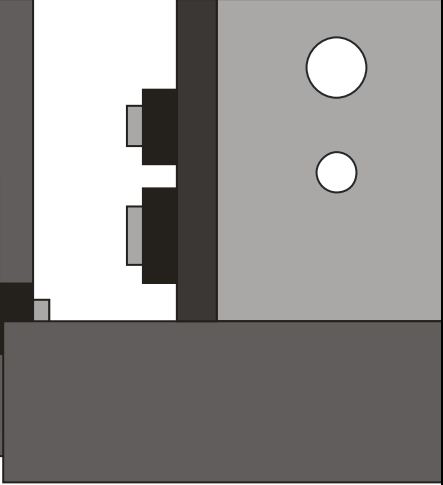
Grip	Sections	Top View	Side View
Type I Staggered connection	Angle		

Table 14: Type II Grip Diagrams

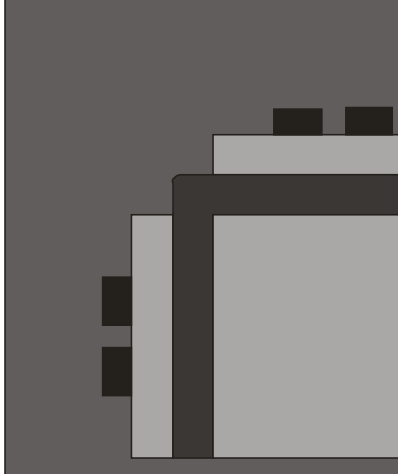
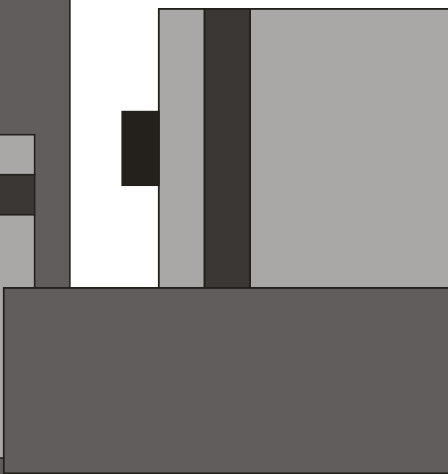
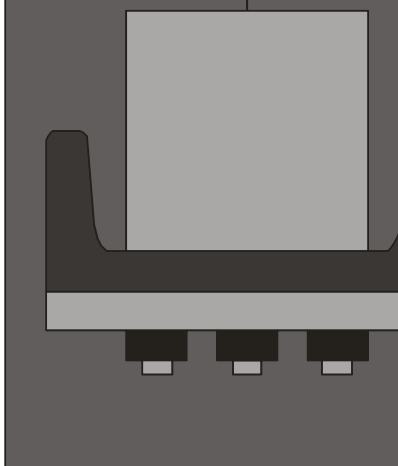
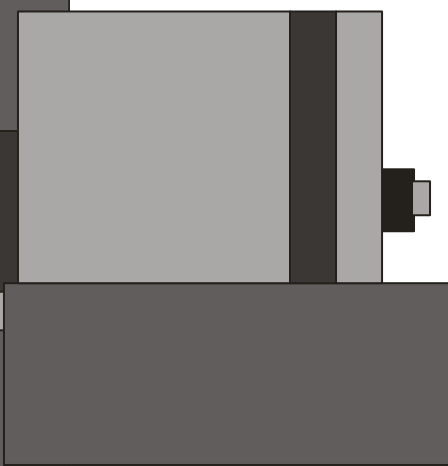
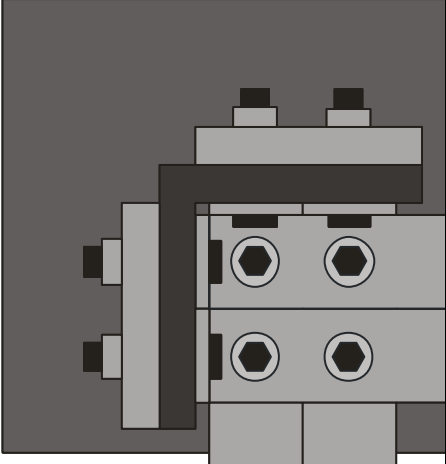
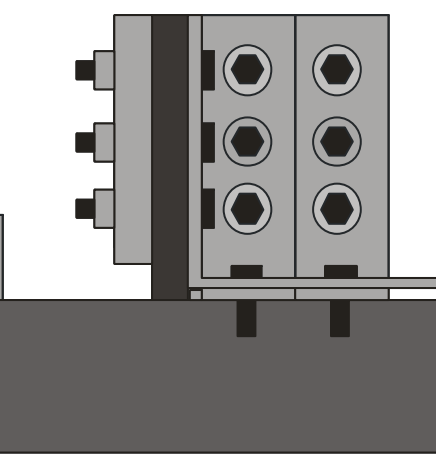
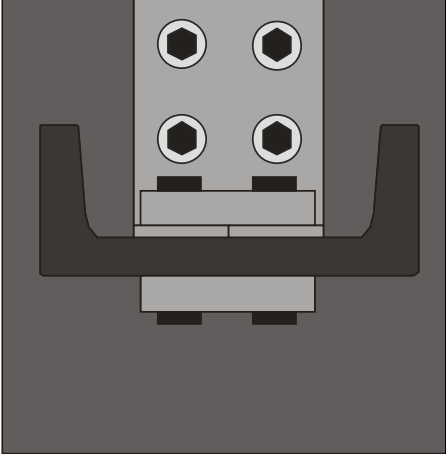
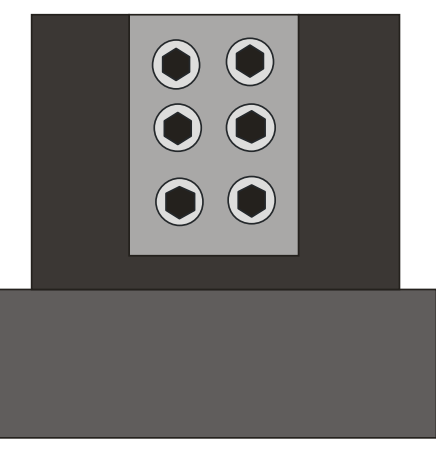
Grip	Sections	Top View	Side View
Type II Collinear connection	Angle		
	Channel		

Table 15: Type III Grip Diagrams

Grip	Sections	Top View	Side View
Type III Tied clamp	Angle	 <p>The top view shows a central grey component with four hexagonal holes arranged in a 2x2 grid. This component is mounted on a dark grey base. To the left, a dark grey L-shaped bracket is attached to the side of the central component. Two small black rectangular protrusions are visible at the top of the central component.</p>	 <p>The side view shows the central grey component with four hexagonal holes in a 2x2 grid. It is mounted on a dark grey base. To the left, a dark grey vertical plate is attached to the side of the component. Three small black rectangular protrusions are visible on the left side of the vertical plate. A thin horizontal line extends from the right side of the central component.</p>
	Channel	 <p>The top view shows a central grey component with four hexagonal holes in a 2x2 grid. This component is mounted on a dark grey base. A dark grey U-shaped channel is attached to the bottom of the central component. Two small black rectangular protrusions are visible at the bottom of the central component.</p>	 <p>The side view shows the central grey component with four hexagonal holes in a 2x2 grid. It is mounted on a dark grey base. A dark grey U-shaped channel is attached to the bottom of the central component. Two small black rectangular protrusions are visible at the bottom of the central component.</p>

APPENDIX C

TRC STRUCTURAL SHAPES FAILURE MODES

Table 16: Failure modes of TRC angles

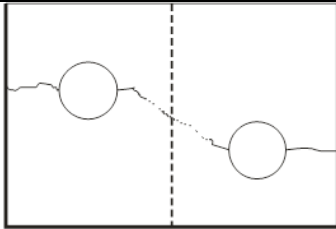

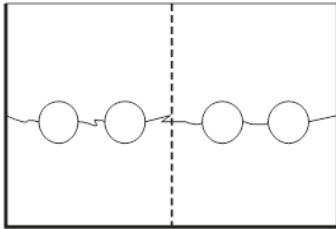

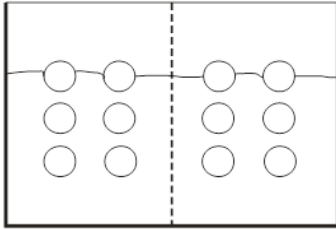

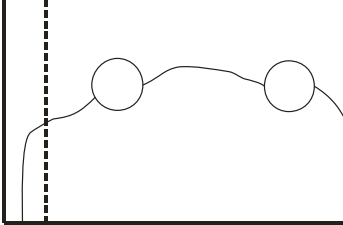

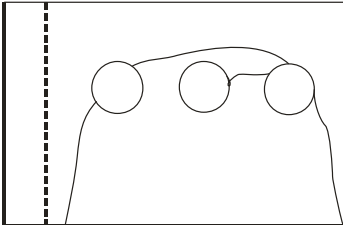

Grip Type	No. of Bolts per leg	Bolt Diameter (mm)	Bolt Spacing		Mode of Failure	Cracking Pattern
			Longitudinal (mm)	Lateral (mm)		
I	1	12	-	-	<p>Bolt Bearing Failure</p> 	
II	2	10	-	26	<p>Tensile Bearing Failure</p> 	
III	6	8	25	32	<p>Tensile Bearing Failure</p> 	

Table 17: Failure modes of TRC channels

Grip Type	No. of Bolts per leg	Bolt Diameter (mm)	Bolt Spacing		Mode of Failure	Cracking Pattern
			Longitudinal (mm)	Lateral (mm)		
II	2	10	-	57	Shear Block Failure 	
	3	10	-	28	Shear Block Failure 	
III	6	8	25	32	Tensile Bearing Failure 